SACLANTCEN REPORT
serial no: SR-294

SACLANT UNDERSEA RESEARCH CENTRE REPORT

OCEANOGRAPHIC MEASUREMENTS OF THE WEST BLACK SEA: NOVEMBER 26 TO DECEMBER 14, 1995

D. Di Iorio, T. Akal, J. Sellschopp
P. Guerrini, H. Yüce, E. Gezgin

June 1998

The SACLANT Undersea Research Centre provides the Supreme Allied Commander Atlantic (SACLANT) with scientific and technical assistance under the terms of its NATO charter, which entered into force on 1 February 1963. Without prejudice to this main task – and under the policy direction of SACLANT – the Centre also renders scientific and technical assistance to the individual NATO nations.

Report no. changed (Mar 2006): SR-294-UU

SACLANT Undersea Research Centre
Viale San Bartolomeo 400
19138 San Bartolomeo (SP), Italy

tel: +39-0187-540.111
fax: +39-0187-524.600

e-mail: library@saclantc.nato.int

NORTH ATLANTIC TREATY ORGANIZATION

Oceanographic Measurements of the West Black Sea: November 26 to December 14, 1995

D. Di Iorio, T. Akal, J. Sellschopp,
P. Guerrini, H. Yüce, E. Gezgin

The content of this document pertains to work performed under Project 022-1 of the SACLANTCEN Programme of Work. The document has been approved for release by The Director, SACLANTCEN.

Jan L. Spoelstra
Director

intentionally blank page

Oceanographic Measurements of the West Black Sea: November 26 to December 14, 1995

D. Di Iorio, T. Akal, J. Sellschopp, P. Guerrini, H. Yüce*, E. Gezgin**

Executive Summary:

This report describes the oceanographic measurement program carried out as part of SACLANTCEN's Black Sea 1995 project in collaboration with the Turkish Navy Department of Navigation, Hydrography and Oceanography. An extensive survey was carried out in the Black Sea exit region of the Strait of Istanbul (Bosporus). The data described in this report differ to previous studies in this area as it was possible to obtain detailed bathymetry from swath mapping and thus track Mediterranean water into the Black Sea using high frequency echo soundings and (conductivity, temperature, depth) CTD profiling. Moored instrumentation recorded detailed Mediterranean inflow characteristics showing that the flow is intermittent.

Mediterranean Sea water flowing into the Black Sea forms a thin dense layer on the Black Sea continental shelf. The sound speed characteristics of this thin layer are such that the sea bottom can be masked. This localized effect of masking the sea bottom for a range of acoustic propagation angles may affect propagation loss and reverberation modelling. Ray tracing from a forward looking sonar show that the critical angle is 75° from the vertical. This implies that acoustic transmission into the Mediterranean water is essentially zero for incident ray angles greater than 75°. This characteristic makes it difficult to detect underwater objects on the sea floor. Sonars closest to the sea surface will transmit more energy through the Mediterranean layer than sonars with variable depth capability. In the event of a mine threat in this area, mine hunting operations are likely to be ineffective.

* Eng. Capt., Assoc. Prof. Dr. Hüseyin Yüce, TUNA
Turkish National Representative, SACLANTCEN
Scientific Committee of National Representatives,
Head of the Department of Navigation, Hydrography and Oceanography,
Istanbul, TURKEY
** Lt. Erhan Gezgin,
Department of Navigation, Hydrography and Oceanography,
Istanbul, TURKEY

intentionally blank page

Oceanographic Measurements of the West Black Sea: November 26 to December 14, 1995

D. Di Iorio, T. Akal, J. Sellschopp, P. Guerrini, H. Yüce, E. Gezgin

Abstract:

Mediterranean water inflow into the Black Sea is investigated using acoustic and oceanographic data obtained in the Black Sea exit region. Temporal and spatial variability in the flow and their relation to atmospheric and sea level changes are documented. The turbulent boundary layer formed by Mediterranean flow over the sea bottom results in turbulent mixing because of hydrodynamic instability. The path of Mediterranean Sea water and the spreading on the continental shelf is observed with SWATH bottom bathymetry measurements, high resolution echo soundings and CTD profiles. The dilution of the saline Mediterranean water as it flows and spreads on the shelf is only 6 psu before reaching the continental slope, where it sinks to a depth appropriate to its density. The Mediterranean effluent is then incorporated in the general circulation of the southwestern Black Sea. The eastward circulation of the surface water is observed using satellite imagery and shipboard ADCP.

Contents

List of Figures

List of Tables

intentionally blank page

1

Introduction

The Strait of Istanbul (Bosporus) separates the Black Sea and the Mediterranean Sea, two relatively large inland seas of differing hydrological characteristics (see Figure 1). Flow through the Strait is a classic example of turbulent exchange flow (Tolmazin, 1985). A high velocity surface current with relatively fresh Black Sea water overlies a current running in the opposite direction, transporting the more saline bottom water of the Marmara Sea which is of Mediterranean origin to the Black Sea. Highly saline and dense bottom Mediterranean water flows through an underwater canyon which starts at the southern end of the Strait and extends 20 km into the Black Sea. The Mediterranean bottom water then spreads on the shelf at some 80 m water depth and finally reaches the shelf break and sinks to a depth at which it finds a common density.

The exchange through the Strait of Istanbul (Bosporus) plays an important role in determining the oceanographic properties in the neighbouring basins. The Mediterranean inflow is the only source of ventilation and renewal of anoxic waters of the deep Black Sea. The surplus of fresh water from rivers and precipitation against evaporation keeps the surface layer in the Black Sea relatively fresh and leads to higher outflow through the Bosporus than the average amount of saline Mediterranean water that advances into the Black Sea (Ünlüata et al., 1990). This input/output process satisfies the salt balance within the Black Sea.

This report describes oceanographic measurements taken during a November / December 1995 sea trial in the Black Sea exit region. Collaboration with the Turkish Navy Department of Navigation, Hydrography and Oceanography (TN DNHO) made it possible to obtain a variety of data. The scientific objectives of this sea trial were to obtain detailed bathymetry since available bathymetry was not sufficient, sample the water column to locate the Mediterranean effluent and measure the dilution, obtain flow characteristics of the bottom water and determine if it is continuous or intermittent and to obtain bottom boundary layer turbulence parameters.

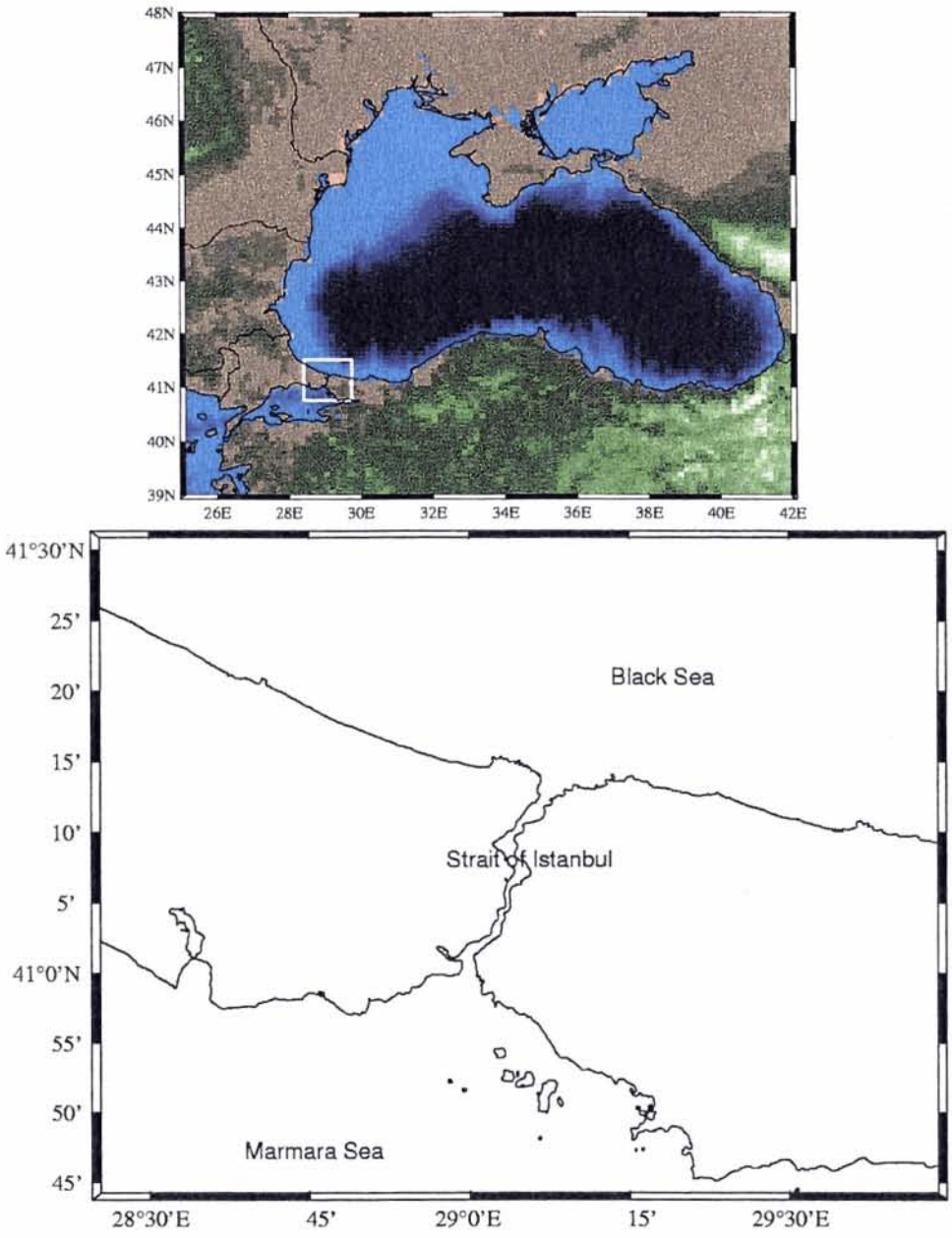

Figure 1 *The Black Sea and Marmara Sea basins. Bathymetry and elevation data are from the ETOPO5 data base; coastline is from the World Vector Shoreline data base.*

2 Experiment

The sea trial in the Black Sea exit region covered a period of 4 weeks in November/December 1995. The NATO Research Vessel (NRV) *Alliance* and the Turkish Navy Survey Ship (TCG) *Çubuklu* were the participating units of the research program. Initially, oceanographic instrumentation were deployed in the Strait of Istanbul (Bosporus) and at the exit region of the Black Sea (see Figure 2). These instruments were used to monitor the exchange of Black Sea and Mediterranean Sea water. Acoustic instruments consisted of a high frequency (307 kHz) acoustic scintillation system for turbulence analysis and a 600 kHz broad band acoustic Doppler current profiler (ADCP) for flow measurements. Two sea level stations at opposite ends of the Strait were used to give relative sea level difference data and a meteorological station monitored wind velocity and air pressure. In order to obtain temporal variability in temperature and salinity, TCG *Çubuklu* was anchored in the vicinity of the ADCP for a 36 h period obtaining conductivity, temperature and depth (CTD) profiles every half hour; once an hour the CTD was lowered to 60 m depth to obtain a 12 min time series. Figure 2 shows a map of the mooring locations in the Strait of Istanbul (Bosporus). Table 1 gives the position of each.

A multi-beam SWATH echo sounder was used to obtain detailed bottom bathymetry because Mediterranean flow is determined by the bathymetry. For most of the experiment NRV *Alliance* and TCG *Çubuklu* surveyed the continental shelf, obtaining CTD profiles along the canyon and a 2 mile grid on the shelf in order to locate the Mediterranean effluent and measure the dilution. A high resolution, high frequency (120 kHz) echo sounder was used for two dimensional imaging of the two layer flow structure. Additional CTD measurements of the Mediterranean bottom water were made according to the imaging results.

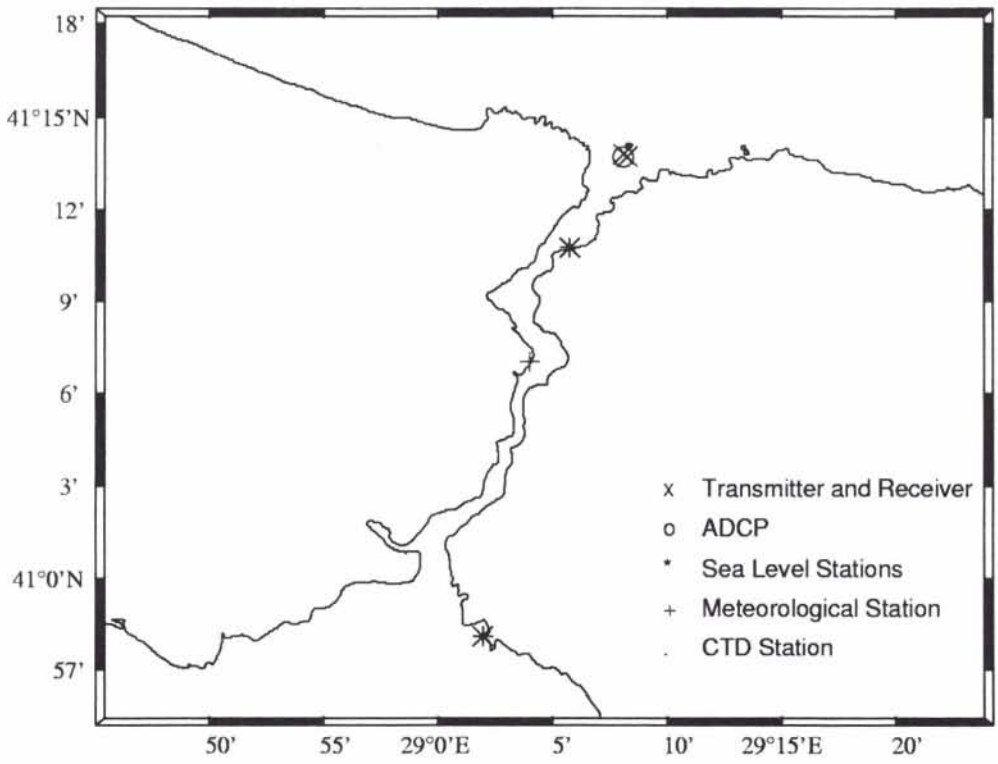

Figure 2 *Strait of Istanbul (Bosporus) showing the location of the ADCP, the acoustic scintillation transmitter and receiver, two sea level stations, a meteorological station and TCG Çubuklu CTD station.*

Instrument	Latitude	Longitude
ADCP	41° 13.682' N	29° 8.079' E
Scintillation transmitter	41° 13.774' N	29° 8.083' E
Scintillation receiver	41° 13.689' N	29° 8.250' E
Sea level station (Anadolukavak)	41° 10.750' N	29° 5.750' E
Sea level station (Fenerbahce)	40° 58.100' N	29° 1.950' E
Meteorological station	41° 7.000' N	29° 4.000' E
CTD station	41° 14.050' N	29° 8.317' E

Table 1 *Instrument locations in the Strait of Istanbul (Bosporus) (see Figure 2).*

3

Moored Instrumentation

3.1 Acoustic Doppler current profiler

The acoustic Doppler current profiler was bottom mounted at depth 72.2 m. The physical characteristics of this instrument allow measurement close to the bottom boundary (first sample is 2.2 m from the bottom). Table 2 lists the relevant set up parameters. The ADCP transmits once every 12 s and obtains a 40 transmission ensemble average every 10 min. Three components of current are obtained: N-S, E-W and vertical at 1 m bin interval for 50 bins.

As the ADCP is moored in a location where Mediterranean flow is confined within a canyon oriented approximately 38^o True North (as will be shown), the component of flow parallel and perpendicular to this direction is calculated and plotted in Figure 3. Positive values correspond to flow toward the northeast and northwest for the along and cross stream current component respectively (a right handed coordinate system). White is used to denote zero current. Maximum Mediterranean water inflow was 80 $cm\ s^{-1}$ occurring between depths 50-60 m, and maximum Black Sea water outflow was 30 $cm\ s^{-1}$ over the entire layer. The most striking feature of this two layer flow dynamics is the change in thickness of the Mediterranean layer over a time scale of 6 days. The cross stream component of the Mediterranean water shows two distinct layers flowing in opposite directions as will be discussed.

Parameter	quantity
Start time	26-NOV-1995 13:04 UTC
End time	13-DEC-1995 11:34 UTC
Frequency	600 kHz
Transmission rate	0.08333 Hz
Ensemble average	40 transmissions
Ensemble interval	10 min
Bin length	1 m
Total bins	50
Depth range	21 to 70 m

Table 2 *ADCP instrument parameters.*

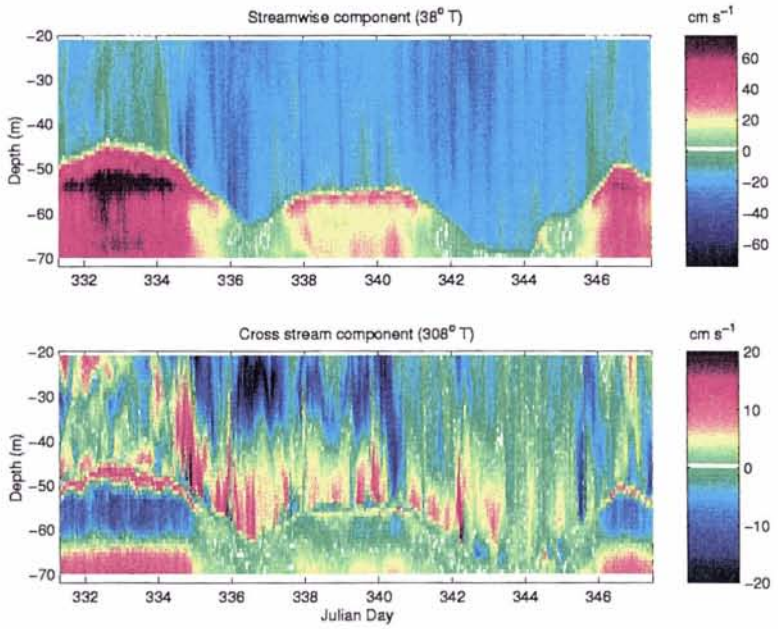

Figure 3 *The component of flow resolved along 38° True North and 128° True North. Mediterranean flow into the Black Sea (North) is positive and Black Sea outflow (South) is negative; westward flow is positive and eastward flow is negative.*

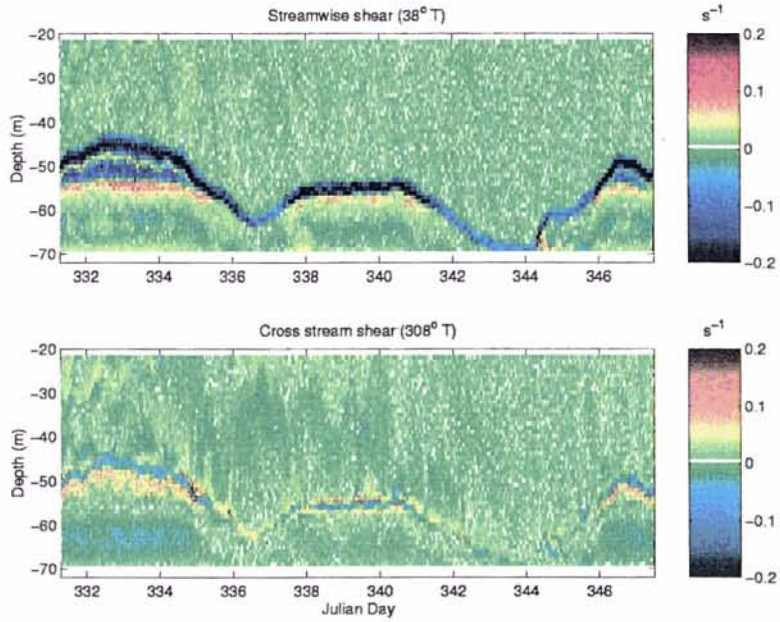

Figure 4 *Current shear resolved along and perpendicular to the canyon.*

The temporal change in interface depth is most easily seen by the shear shown in Figure 4. The shear is calculated at 1 m depth intervals. Maximum shear observed was $-0.5s^{-1}$ in the along stream component and $0.15s^{-1}$ in the cross stream component. The temporal change in interface depth (where the streamwise shear is maximum), as will be shown, is a result of blockage of the Mediterranean flow as a result of sea level differences, which in turn depend on wind speed and freshwater input (Yüce, 1996). When there is lower layer blockage there is extreme southwesterly flow in the upper layer.

As Mediterranean flow is confined between two boundaries (the bottom boundary below and Black Sea water above), a balance of friction, Coriolis force and pressure gradient will result in a cross stream shear over the full thickness of the Mediterranean layer. Figure 5 shows profiles of the along and cross stream current components averaged over 1.2 Julian days when the Mediterranean flow was maximum (between Julian day 332 6:35 and 333 10:54) together with the current vectors as a function of depth. As the bottom boundary and interface are approached, the current swings to the left (i.e. westward) resulting in Ekman-like spirals. This spiraling circulation pattern may also be the result of the complex bathymetry that exists within the canyon just South of the mooring location (as will be seen in Section 4.1).

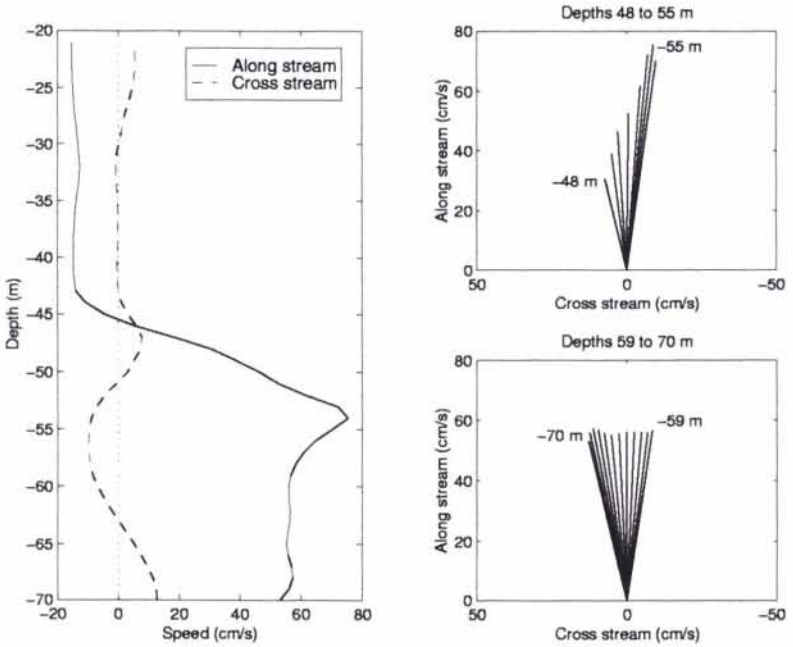

Figure 5 *Average current profile resolved along (solid curve) and across (dotted curve) the canyon together with current vectors at 48 - 55 m and 59 - 70 m.*

3.2 Meteorological and sea level data

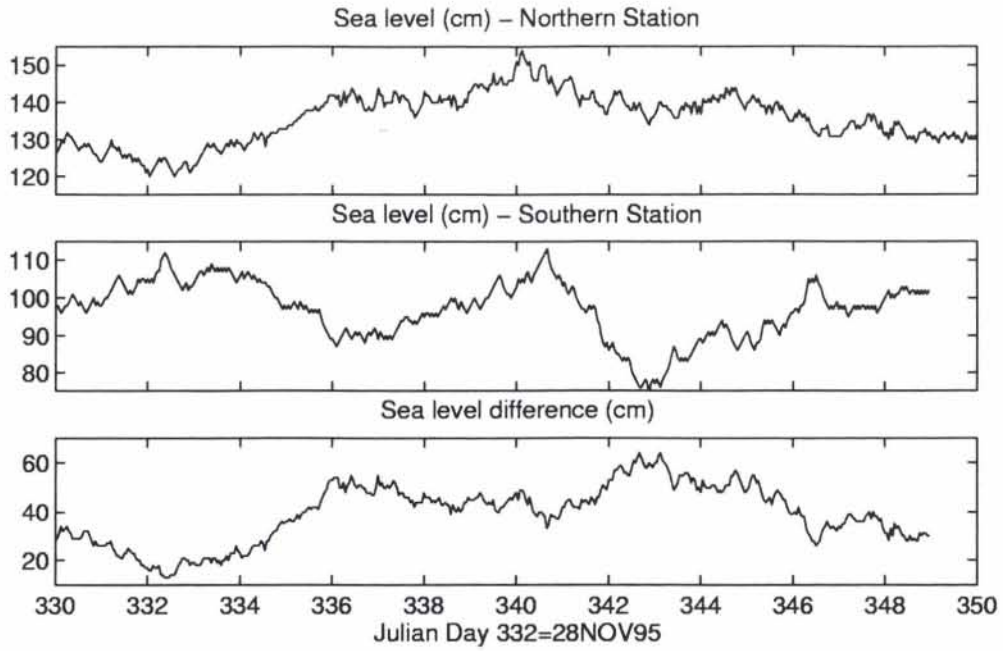

Figure 6 *Sea level heights at the northern and southern station together with the difference.*

The sea level data for the Black Sea and Marmara Sea basins are shown in Figure 6. The relative difference between the northern (Anadolukavak) and southern (Fenerbahce) station shows values that are high enough to cause blockage of the Mediterranean outflow. In fact, when the relative sea level difference is greater than 40 cm the ADCP data in Figure 3 shows the interface well below the sill depth of 60 m thus causing blockage of the Mediterranean outflow. Oğuz et al. (1990) show from their model results that when the absolute sea level difference exceeds 45 cm, transport in the lower layer vanishes.

Meteorological data during the experimental period are shown in Figure 7(a) and (b) from the moored meteorological station and from the Meteo system on board NRV *Alliance* respectively. The air pressure data for NRV *Alliance* and the station show an unexplained difference. The temperature from the station shows diurnal oscillations associated with heating and cooling of the land. Positive (negative) wind vectors indicate wind from the North (South). The wind speeds from the station (maximum 6 $m\ s^{-1}$) are questionable as higher levels were observed during the course of the experiment in the Black Sea exit region (10 $m\ s^{-1}$). The placement of the meteorological buoy within the Strait of Istanbul (Bosporus) is not representative of the conditions within the Black Sea. The sea level difference during this time is closely related to changes in barometric pressure and wind. Time delays may exist

(a)

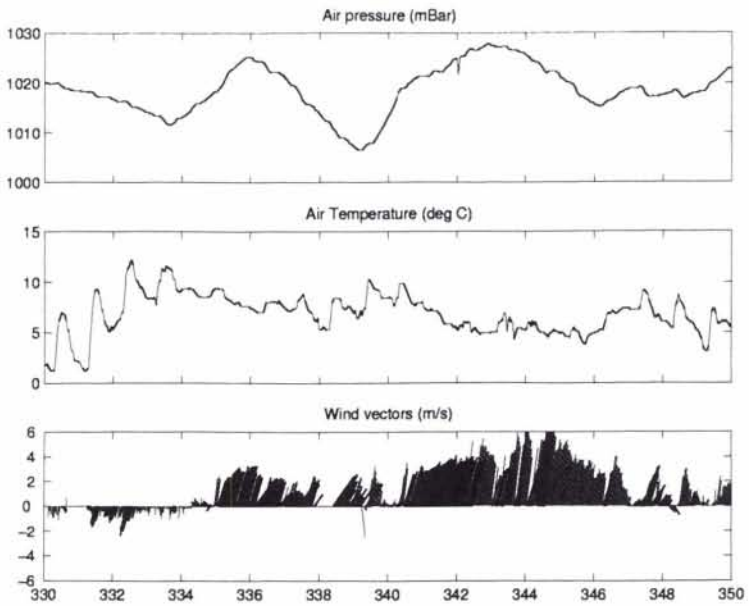

(b)

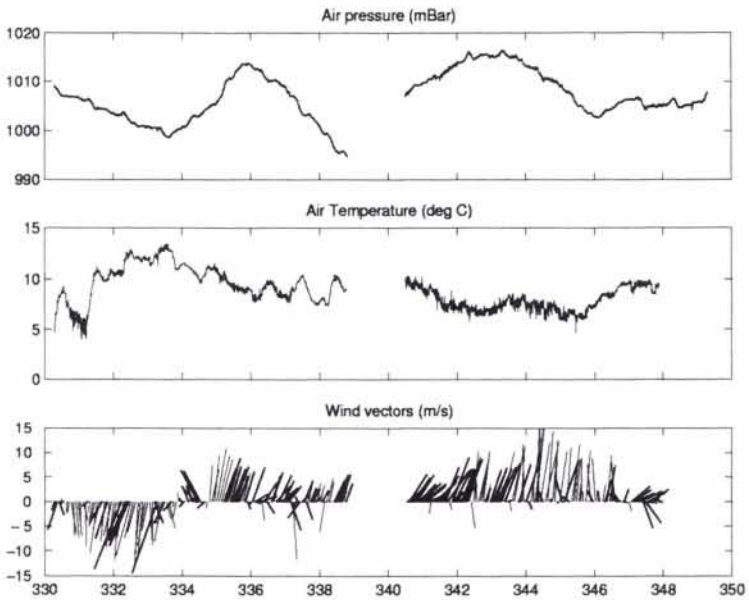

Figure 7 *Meteorological data showing air pressure, temperature and wind vectors from (a) the meteorological station and (b) the Meteo system on NRV Alliance.*

because of the response time required for the water masses to react to meteorological changes.

3.3 CTD time series

TCG *Çubuklu* obtained CTD time series at an anchored station near the ADCP and scintillation system (see Figure 2). These time series consisted of profiles approximately every half hour and a 12 min time series of oceanographic properties once an hour at 60 depth. This temporal variability in temperature and salinity structure is used to determine the degree of mixing that takes place in the dense lower layer and at the interface of the two layers. The 60 m depth was chosen to correspond with the acoustic propagation axis of the scintillation system.

Figure 8 shows colour images of the temperature and salinity profiles over time with contours superimposed. The shallow thermocline at 15 m depth shows vertical variations possibly associated with advection of imperfectly mixed water. During this 36 h time series the interface has increased in thickness by 4 m as a result of mixing at location or advection of mixed water. Also, the salinity contour of 18 psu becomes shallower, indicating that more salt is entrained into the Black Sea water; in contrast there is a decrease in salt content in the Mediterranean effluent. For example, calculations of the depth integrated salinity show that the Black Sea water (depth 1-48.5 m) salinity increases by 0.4 psu and that Mediterranean effluent (depth 48.75-64.25 m) decreases by 0.6 psu. This salinity variability is associated with advection and local mixing.

The temperature-salinity relation for the time series profiles is shown in Figure 9 with contours of σ_t and sound speed evaluated at 0 dbar pressure; pressure effects on sound speed over 60 m depth is approximately 1 $m\ s^{-1}$ and therefore has been ignored for these contours. The sound speed difference between Black Sea and Mediterranean Sea water is 40 $m\ s^{-1}$ and the density difference is 14 $kg\ m^{-3}$. Because of the large salinity range, it is interesting to note that salinity effects on sound speed in this environment are important as the contours are diagonal instead of horizontal.

The CTD profiles in conjunction with current profiles from the ADCP give a measure of hydrodynamic stability. This is parameterized by the gradient Richardson number,

$$\begin{aligned} \mathrm{Ri} &= N^2 \left[\left(\frac{dU}{dz} \right)^2 + \left(\frac{dV}{dz} \right)^2 \right]^{-1}, \qquad (1) \\ N^2 &= -\frac{g}{\rho_o} \frac{d\rho_o}{dz}. \end{aligned}$$

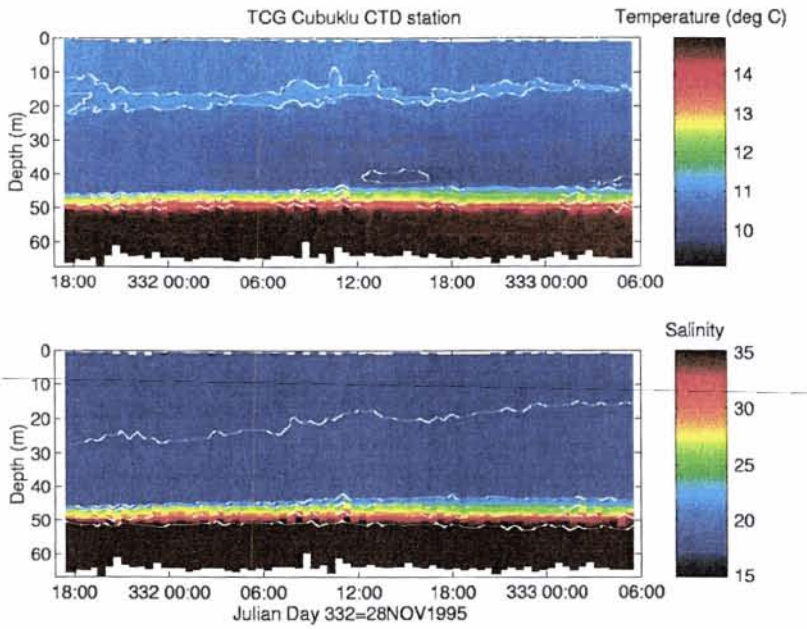

Figure 8 *Temperature and salinity profile time series taken by TCG Çubuklu at the moored station. Contours for temperature are [10, 11, 12, 13, 14 °C] and for salinity [18, 20, 25, 30, 35 psu].*

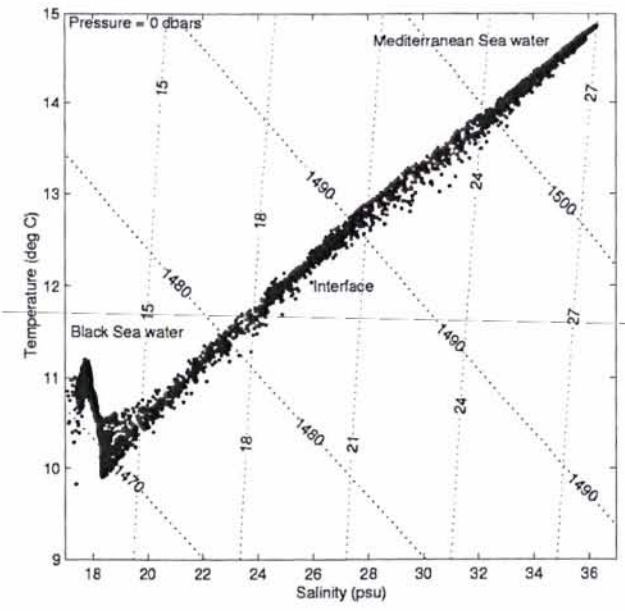

Figure 9 *Temperature versus salinity for the profiles shown in Figure 8. Contours of σ_t and sound speed evaluated with no pressure effects are also shown.*

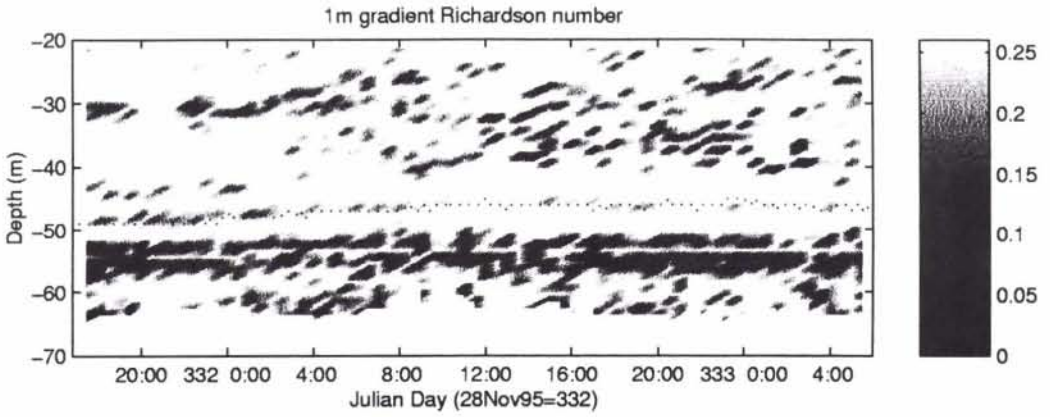

Figure 10 *The 1 m gradient Richardson number as a function of depth and time.*

where the mean flow as a function of depth resolved along and across the canyon is U and V respectively. The Brunt-Väisälä frequency is $N/(2\pi)$, ρ_o is the mean density as a function of depth and g is gravity. If the gradient Richardson number becomes large, turbulence is suppressed as the density gradient stabilizes variations caused by current shear; if the gradient Richardson number Ri ≤ 0.25 then shear instabilities give rise to turbulent mixing (Monin and Ozmidov, 1985).

From our time series measurements we compute the 1 m gradient Richardson number as a function of depth and time. The results are shown in Figure 10 with the interface depth shown as a dotted line. Grey shading indicate regions where Ri≤ 0.25. Initially when the interface thickness is small, Ri < 0.25 indicating that shear instabilities give rise to mixing of the two water masses. Later as the interface thickens, Ri becomes greater than 0.25 indicating stability across the interface. Within the Mediterranean layer between depths 50-60 m the Richardson number is consistently $0 <$ Ri < 0.25 as the stratification is weak and the shear strong.

Figures 11 and 12 show 12 min temperature and salinity time series respectively during a 36 h period at a depth of approximately 60 m which is well within the Mediterranean layer. During the measurement, the Mediterranean layer increased in thickness by a few metres and the resulting current increased from 0.5 to 0.6 $m\ s^{-1}$. The sampling rate of 5 Hz limits the smallest scale sensitivity to 12 cm during a maximum flow of 0.6 $m\ s^{-1}$. Thus it is the larger scales that are measured. Figure 13 summarizes the data by showing the mean and standard deviation for each 12 min time series. During this period the mean temperature and salinity of the Mediterranean layer at 60 m decreased by 0.2 ^{o}C and 0.6 psu respectively. Also the root-mean-square (rms) variability is somewhat greater at the maximum flow than earlier. It will be shown however that this variability has negligible effect on acoustic forward scatter.

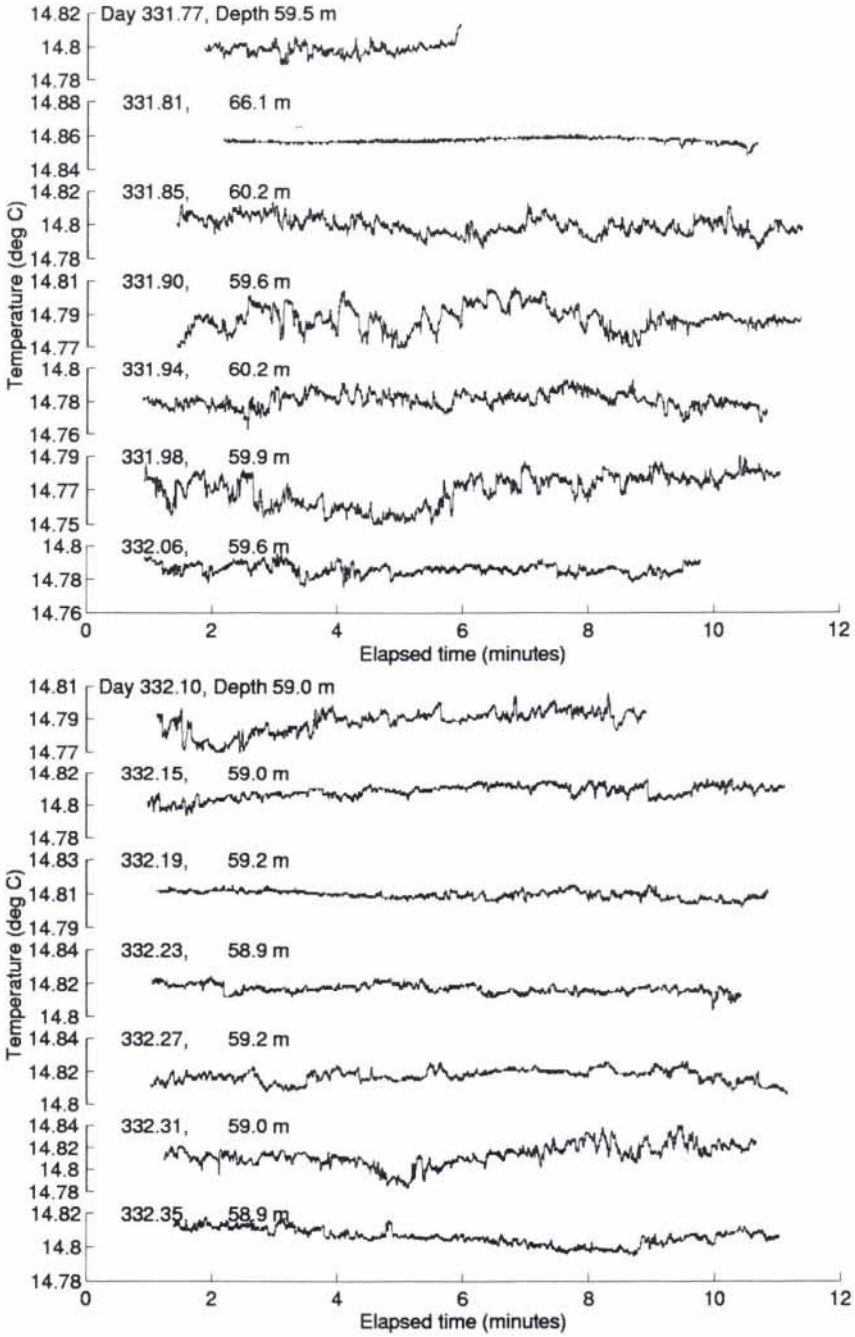

Figure 11 *Temperature time series taken by TCG Çubuklu at their moored station.*

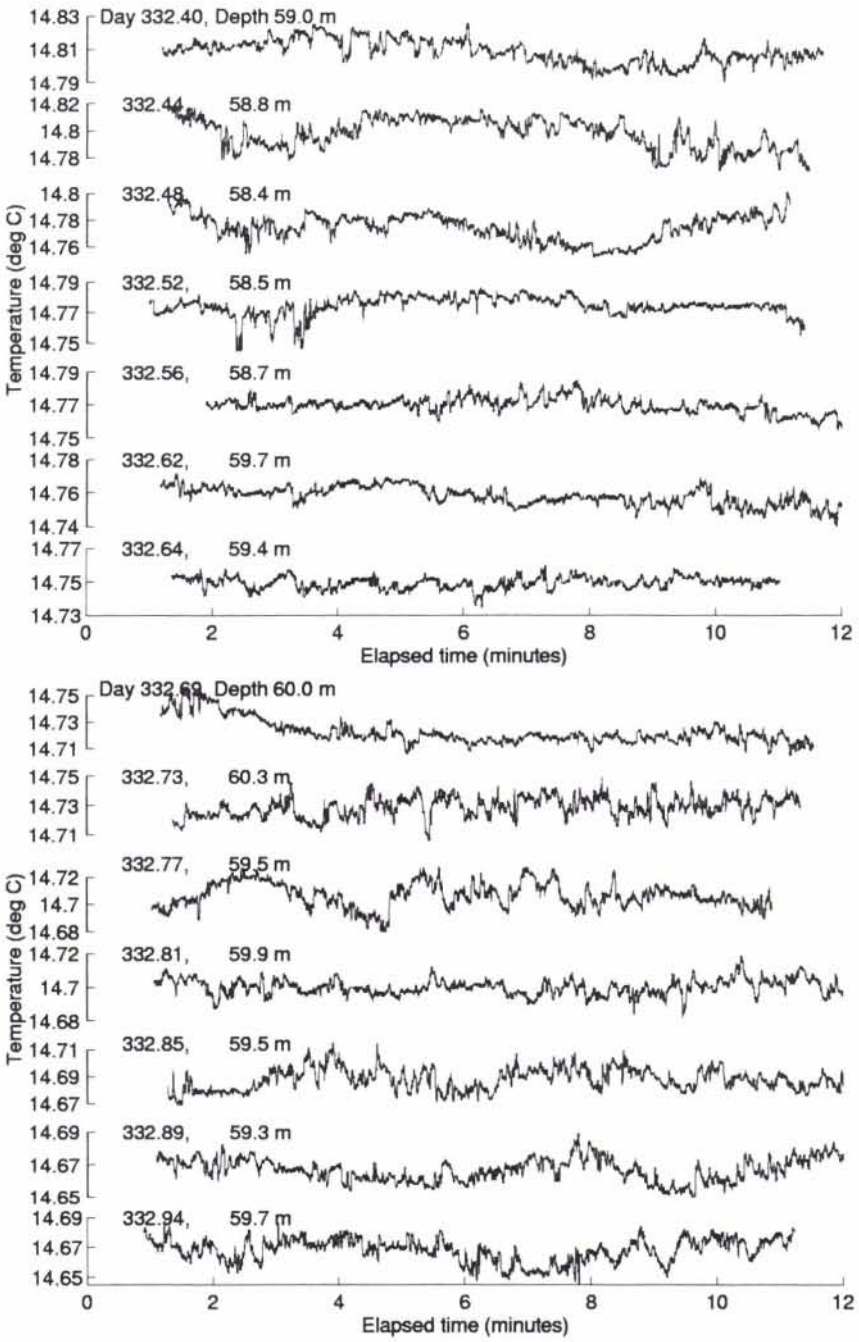

Figure 11 continued.

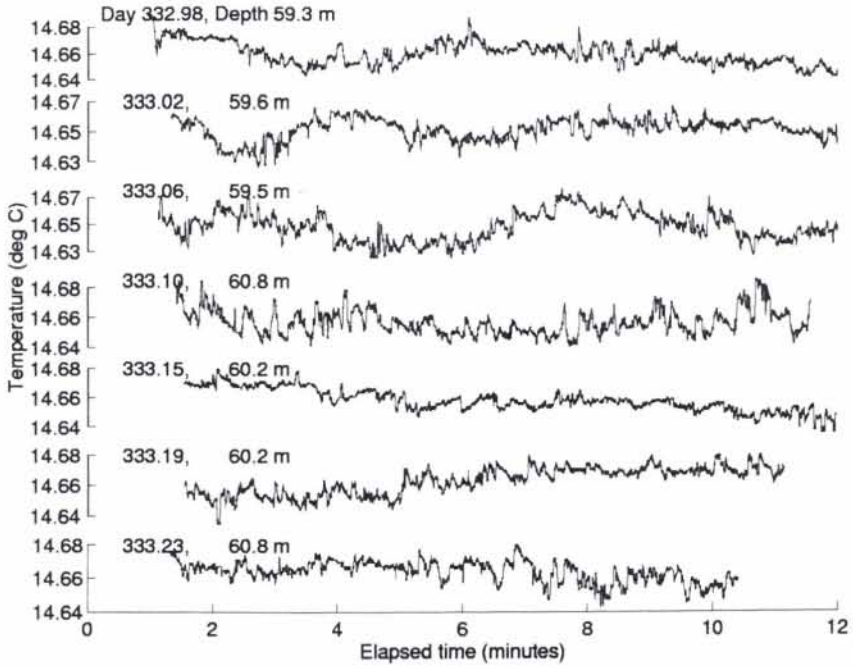

Figure 11 continued.

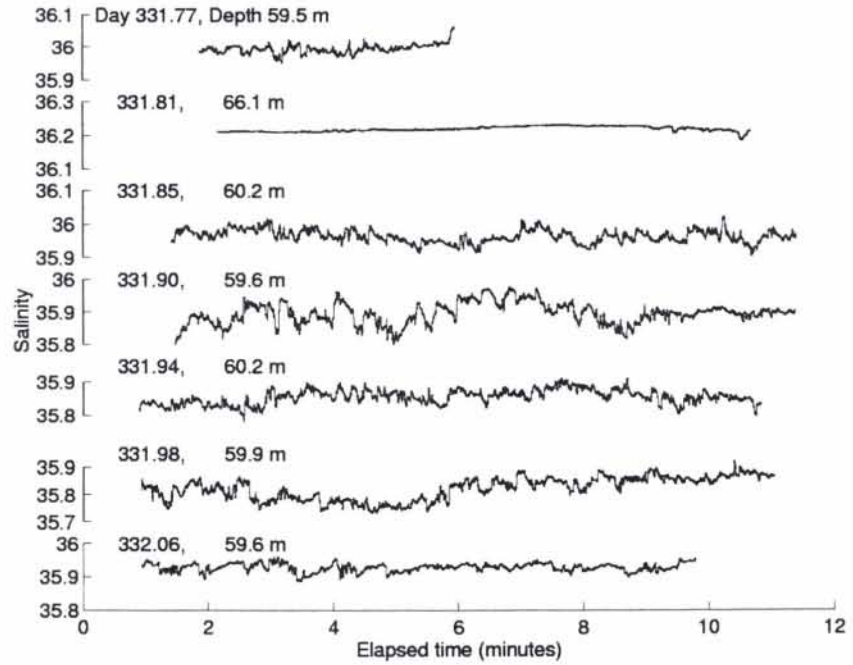

Figure 12 *Salinity time series taken by TCG Çubuklu at their moored station.*

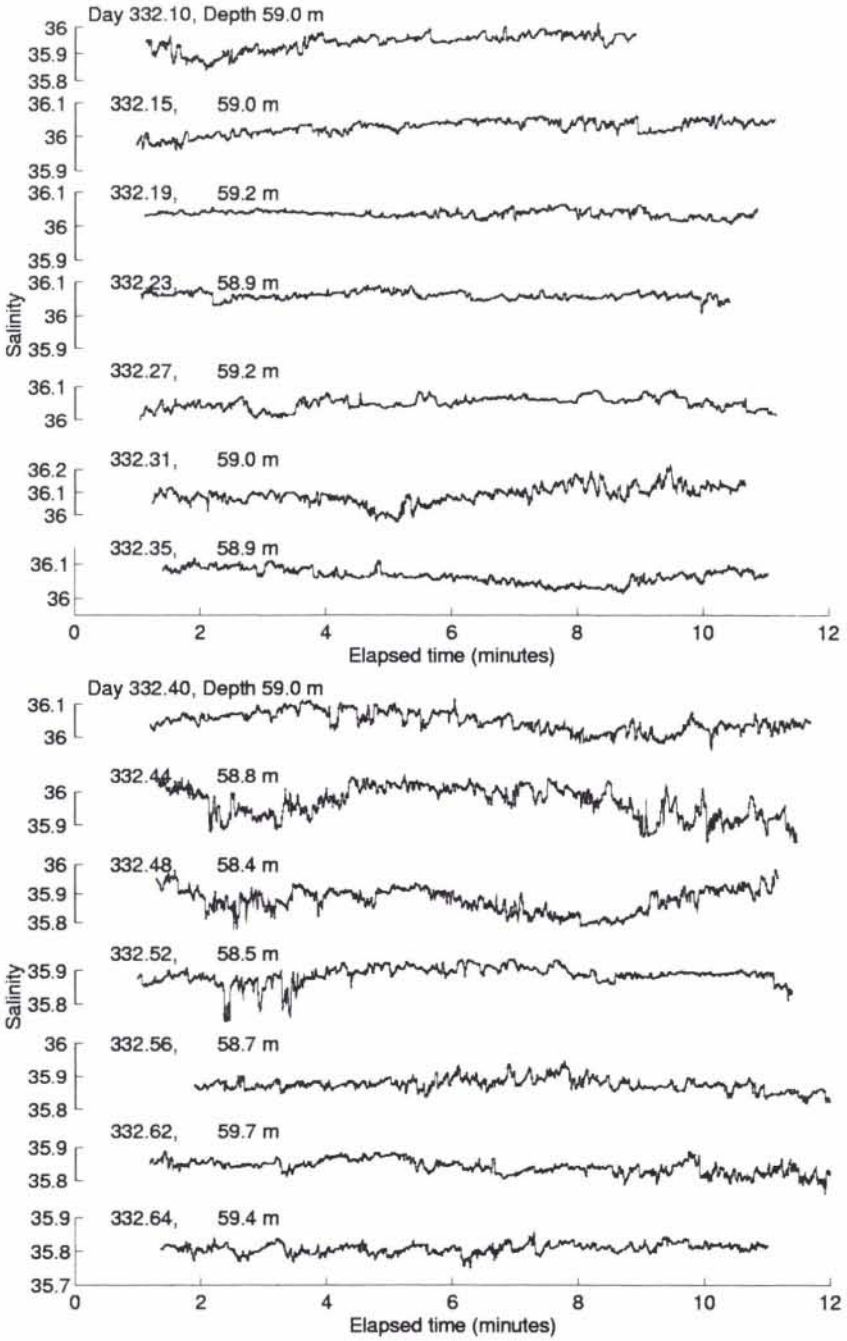

Figure 12 continued.

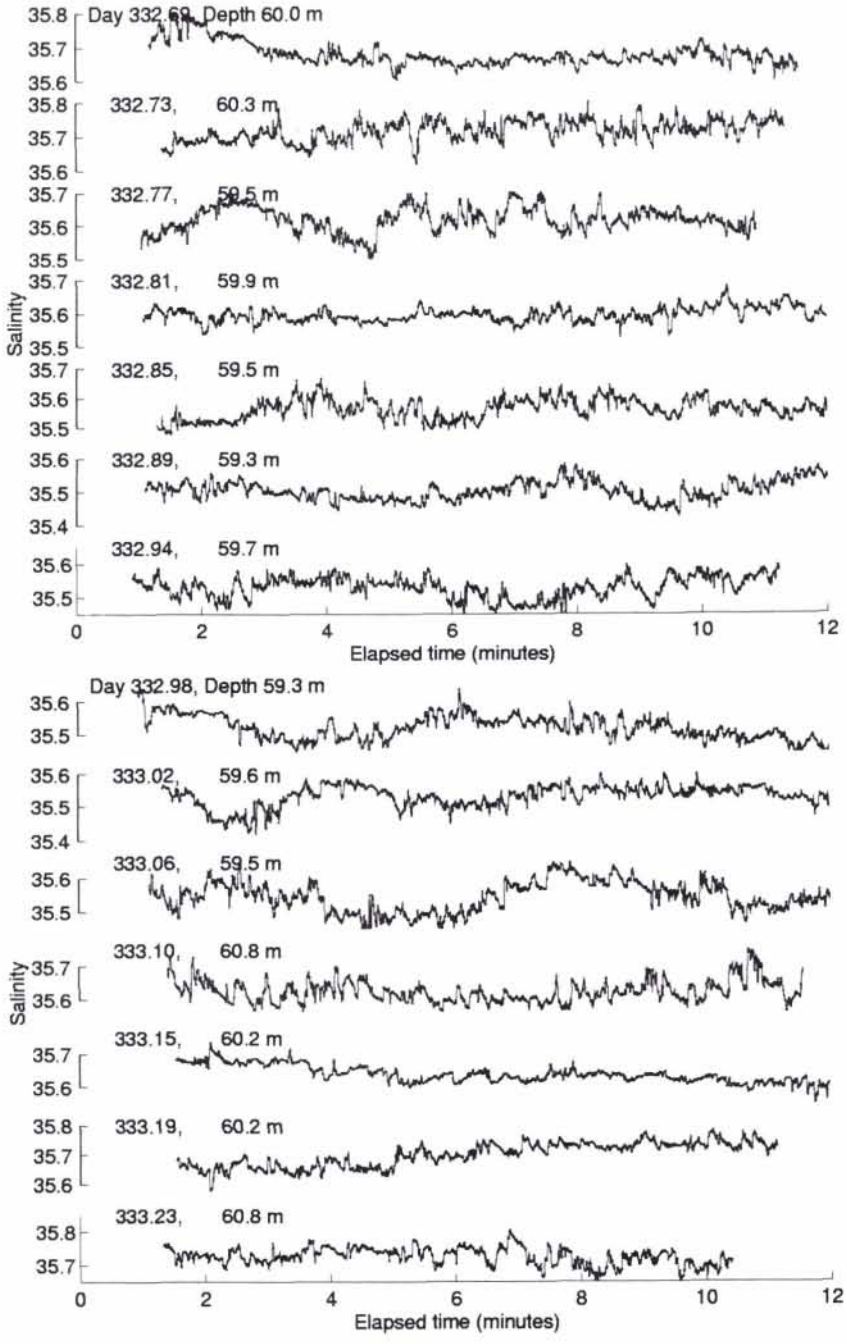

Figure 12 continued.

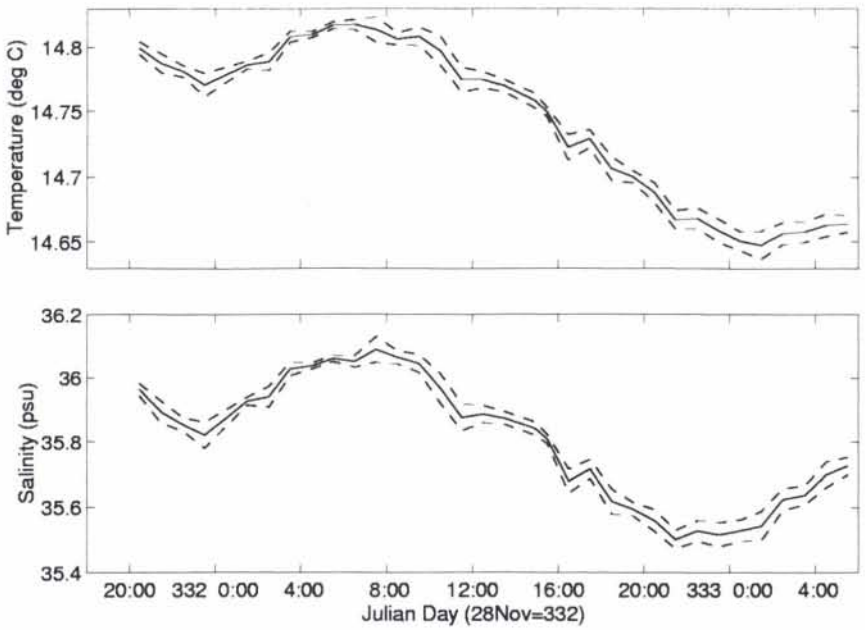

Figure 13 *Mean and standard deviation (rms) of the temperature and salinity time series shown in Figures 11 and 12.*

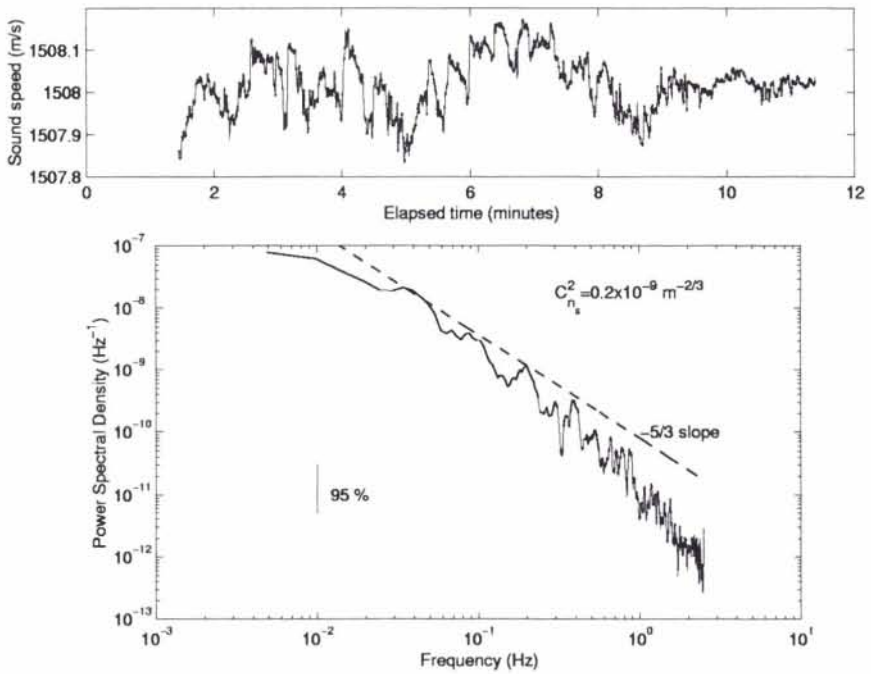

Figure 14 *A sample sound speed time series together with the frequency spectrum for the refractive index fluctuations.*

The refractive index defined as $n = c_o/c$, where c_o is the mean sound speed dependent on temperature and salinity (scalars), can be separated into mean and fluctuating components $(1 + \eta_s)$ in order to describe the statistics. Assuming isotropic and homogeneous turbulence the one-dimensional frequency spectrum for the refractive index fluctuations is defined as,

$$F_{\eta_s}(f) = 0.124 C_{\eta_s} (\frac{U}{2\pi})^{2/3} f^{-5/3}, \tag{2}$$

where C_{η_s} describes the level of the refractive index fluctuations from scalars and U is the mean current speed advecting the small scale turbulence. Figure 14 shows a sample sound speed time series with the one dimensional frequency spectrum for the refractive index fluctuations ($\eta_s = -c'/c_o$). A $-5/3$ slope and the 95% confidence interval is plotted to show that the variability can be modelled as described by Eq. (2). The level of the spectrum gives the structure parameter C_{η_s} which will be compared to acoustic forward scatter results in the next section.

3.4 *Acoustic scintillation*

A high frequency (307.2 kHz) battery operated acoustic scintillation system (on loan from the Institute of Ocean Sciences, Sidney, B.C. CANADA) was deployed within the canyon containing Mediterranean sea water. The transmitter array was deployed on the western side and the receiver array on the eastern side separated by 280 m at a depth of 62.5 m. Each array consists of two transducers separated by 0.2 m. In order to keep the transducer array aligned in the direction of flow, a vane and swivel were attached to the mooring (see Figure 15). This allows measurement of current flow perpendicular to the acoustic axis and measurement of turbulent structures as they are advected past the acoustic path.

Each transducer is horizontal omni-directional with a 10° vertical beam width. Short pulses (30 cycles or 0.1 ms) are transmitted with a high repetition rate (16 Hz) and with a delay of 20 ms between the two spatially separated transducers. The receiver unit complex demodulates the signals, digitizes and calculates the acoustic amplitude, phase and travel time for the direct path using quadratic interpolation of the received enveloped. The data are then recorded on flash EPROM recorder cards. Table 3 summarizes the experimental parameters.

Two deployments were made: 4.5 days of continuous data were collected on the first and 8 days of sub-sampled data (20 min of data every hour) on the second. The data covered a variety of oceanographic phenomena. Figures 16(a) and (b) show the ADCP current vectors (with density contours when available) during deployment 1 and 2 respectively.

In order to calculate the amplitude, phase and travel time of the acoustic pulse, it is

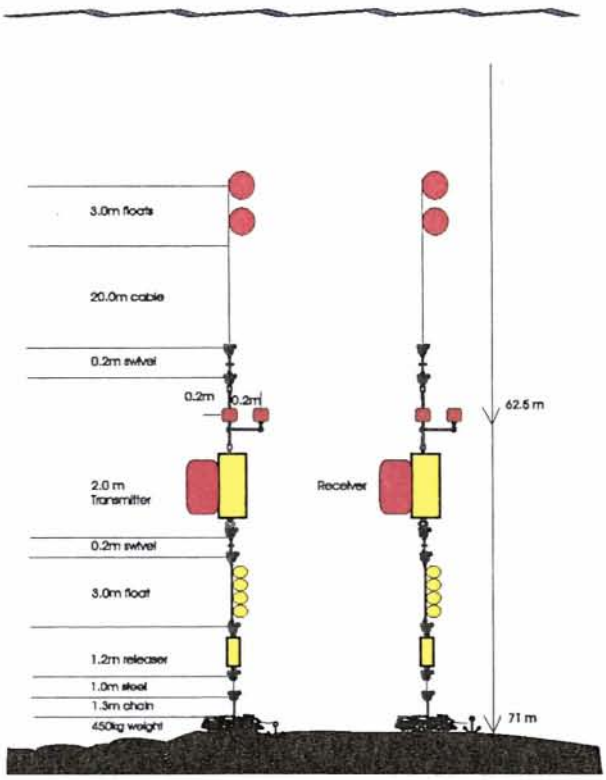

Figure 15 *Acoustic scintillation mooring description.*

Parameter	quantity
Deployment 1	27-NOV-1995 11:00 to 01-DEC-1995 17:00 UTC
Deployment 2	05-DEC-1995 10:00 to 13-DEC-1995 11:30 UTC
Transmission rate	16 Hz
– deployment 1	continuous
– deployment 2	20 min continuous every hour
Frequency	307.2 kHz
Pulse width	0.1 ms
Pulse delay	20 ms
Digitization rate	153600 Hz (1 sample/2 cycles)
Path length	282 m
Propagation direction	124 degrees True
Transducer separation	0.2 m
Depth	62.5 m

Table 3 *Acoustic scintillation instrument parameters.*

(a)

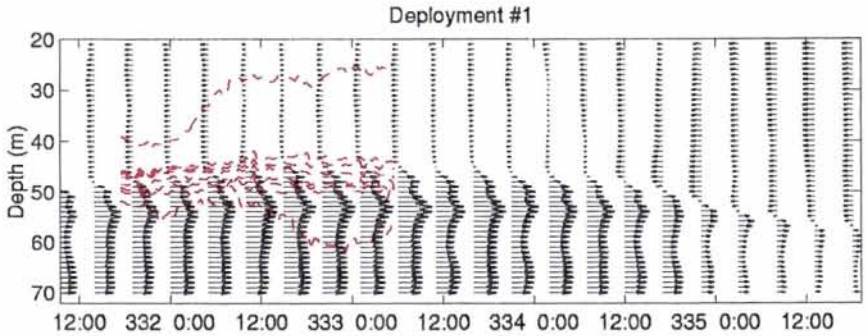

(b)

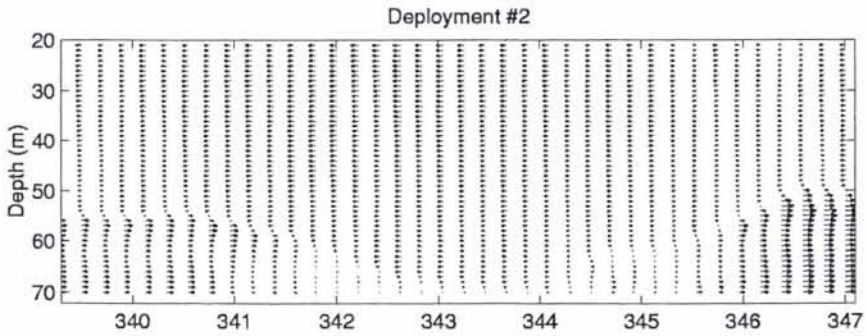

Figure 16 *The ADCP current vectors (with density contours [1014, 1015, 1017, 1019, 1021, 1023, 1025, 1026.75 kg m^{-3}] when available) during (a) deployment 1 and (b) deployment 2.*

crucial that there is path separation at the receiver. For example, eigenray tracing during the oceanographic conditions of deployment 1 with a source and receiver at 62.5 m depth having vertical beam widths of 10^o separated by 280 m, shows that there are only two paths: a direct path and a bottom reflected path. As time separation between the two paths is 0.45 ms and the pulse length is 0.1 ms, path separation is possible. In the second deployment the interface is below the acoustic path for much of the time, thus inhibiting bottom reflection but causing reflection from the interface. Geometry shows that if the interface is at least 4.5 m below the acoustic path, then path separation is possible.

Sample acoustic scintillation data (approximately 2 min) during deployment 1 and 2 are shown in Figure 17(a) and (b) respectively. Sample data is shown at two different times for each deployment. During deployment 1, the Mediterranean undercurrent is strong and then weakens but the interface remains above the acoustic propagation axis. Variability in the amplitude exists during strong flow because of

(a)

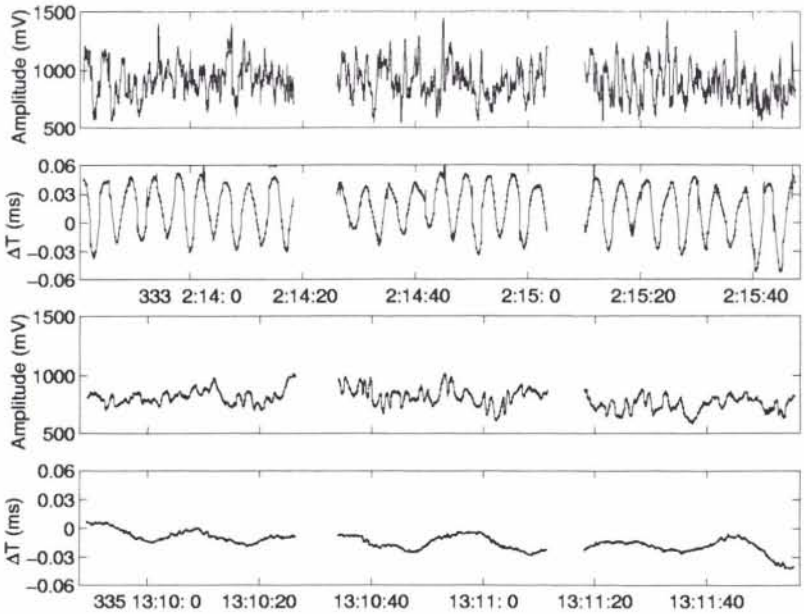

(b)

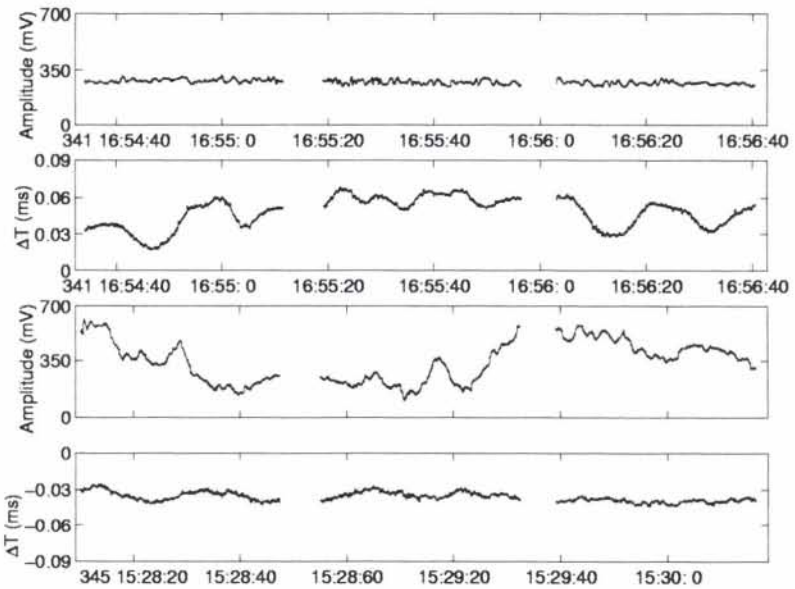

Figure 17 *(a) Sample acoustic scintillation data during deployment 1 when the Mediterranean undercurrent was strong ($U = 0.6m\ s^{-1}$ on day 333.1) and weak ($U = 0.1m\ s^{-1}$ on day 335.5), (b) Sample acoustic scintillation data during deployment 2 just before (day 341.7) and just after blockage (day 345.6).*

the turbulent nature of the flow. The travel time difference between the two parallel paths shows a periodic nature as a result of mooring oscillations. During weaker flow, the amplitude fluctuations and periodicity in the travel time difference weaken. Since the transmission rate was high (16 Hz) and the mooring oscillations small the direct path signal could be tracked. The mooring motion does not affect amplitude variations but the phase and travel time cannot be used as a measurement of medium properties.

Deployment 2 occurred during blockage of Mediterranean water so that the interface passed through the acoustic path. Sample amplitude and travel time difference are given before and after the blockage in Figure 17(b). Before blockage when the Mediterranean flow is suppressed, the amplitude shows little variability but the moorings still undergo oscillations. When the Mediterranean flow is no longer blocked large amplitude changes exist which could be the result of strong mixing between the two very different water masses. During blockage of the Mediterranean inflow, the acoustic data for deployment 2 was of inferior quality. This could be due to a number of reasons: misalignment of the transmitter/receiver arrays because of mooring rotation, inability to track the direct path as the travel time of the acoustic signal changes by up to 3.9 ms and finally, path separation was not possible.

The statistics for the normalized log-amplitude $\chi = \ln(A/ < A >)$ (where A is the acoustic amplitude and $<>$ denotes a time average), allow measurement of oceanographic parameters. For example, Figure 18 shows a short time series (40 s) of the log-amplitude from two parallel acoustic paths (T1/R1 and T2/R2). The time-lagged cross-covariance as shown in the figure, indicates the translation of turbulent structures perpendicular to the two acoustic paths separated by 0.2 m. By measuring the time lag, the current speed is calculated and shown in Figure 19(a) and (b) for each deployment respectively with the ADCP measurement for comparison. Discrepancies between the scintillation technique and the ADCP can arise for a number of reasons. For example, the scintillation measurement is a path average whereas the ADCP measurement is essentially a volume measurement at a point location. Also because of mooring motion, there are changes in the acoustic path separation of 0.2 m.

The log-amplitude variance, σ_χ^2 shows increased variability associated with the increasing current. The large variance observed in deployment 2 could be a result of turbulent mixing between two very different water masses as the Mediterranean flow becomes unblocked.

The level of the effective refractive index fluctuations defined by,

$$C_{n_{eff}}^2 = C_{n_s}^2 + \frac{11}{6} C_{n_v}^2 \tag{3}$$

(Di Iorio and Farmer, 1998) is expressed in terms of the refractive index fluctuations arising from temperature and salinity variability (scalars) and those arising from

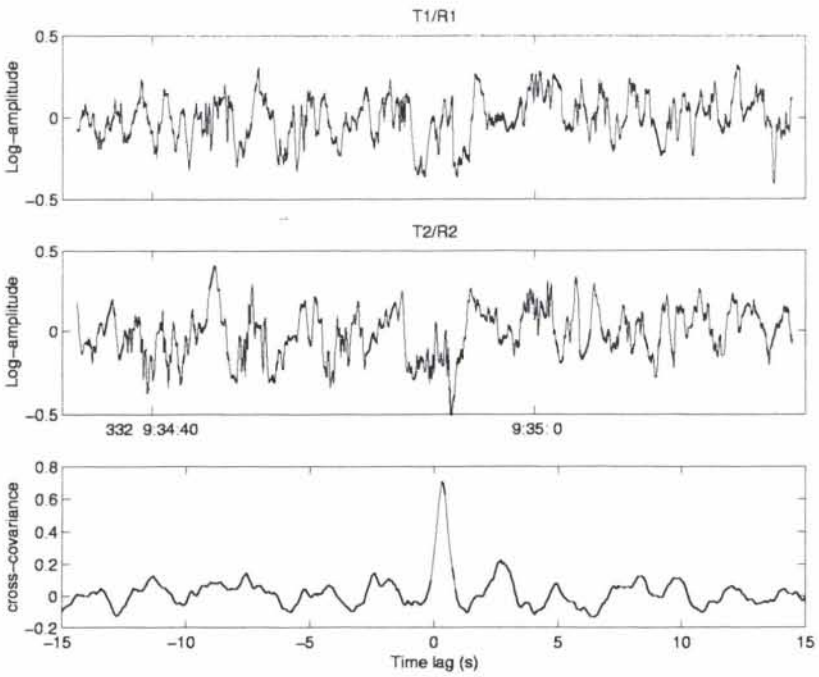

Figure 18 *Log-amplitude for two parallel acoustic paths separated by 0.2 m and the resulting cross-covariance.*

the current variability (vectors). The log-amplitude variance allows measurement of $C^2_{n_eff}$ through the equation,

$$\sigma^2_\chi = 0.124 C^2_{n_{eff}} k^{7/6} L^{11/6}, \tag{4}$$

where k is the acoustic wavenumber and L is the acoustic path length. Note that the acoustic amplitude variability cannot distinguish between fine scale variability from scalars and that from current. The dominant scale size which contributes to the log-amplitude variance discussed by Tatarskii (1971), is the Fresnel radius $\sqrt{\lambda L} = 1.2m$.

Independent measurements of the temperature/salinity structure, as discussed in the previous section, compared with $C^2_{n_eff}$ in Figure 20 shows that the dominant acoustic scattering is from current velocity variability as $C^2_{n_s}$ is at most 10% of $C^2_{n_{eff}}$. Both measurements are sensitive to scale sizes of $\approx 1m$ but the CTD measurement is at a point location and the acoustic measurement is a path average. Current velocity fluctuations arise because of hydrodynamic instability as discussed previously. Within the Mediterranean layer a balance of friction, Coriolis and pressure gradient forces give rise to the resulting flow pattern.

As velocity fluctuations dominate the acoustic scattering, some interesting oceanographic parameters describing the turbulent boundary layer can be calculated. For

(a)

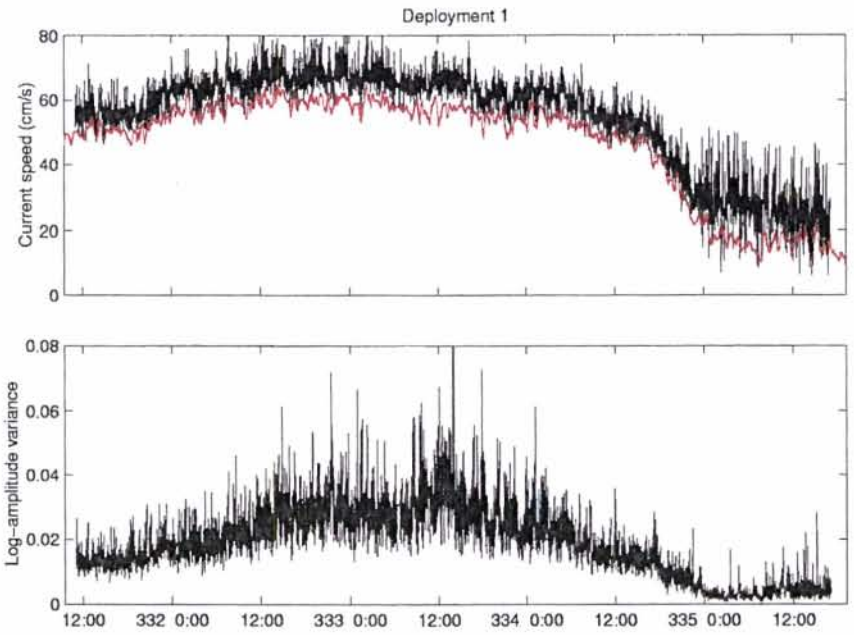

(b)

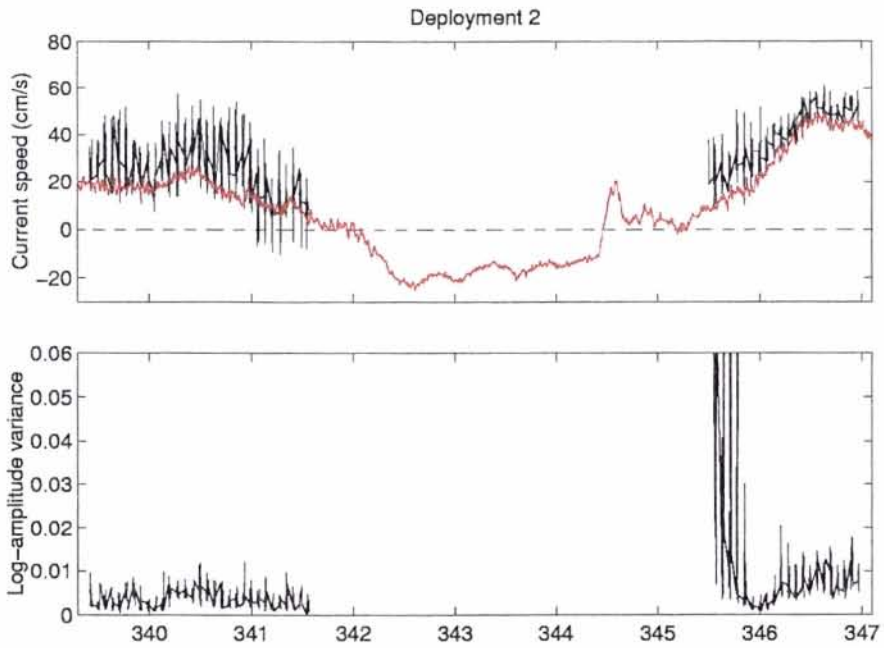

Figure 19 *Current speed measured using acoustic scintillation and ADCP and the log-amplitude variance for (a) deployment 1 and (b) deployment 2.*

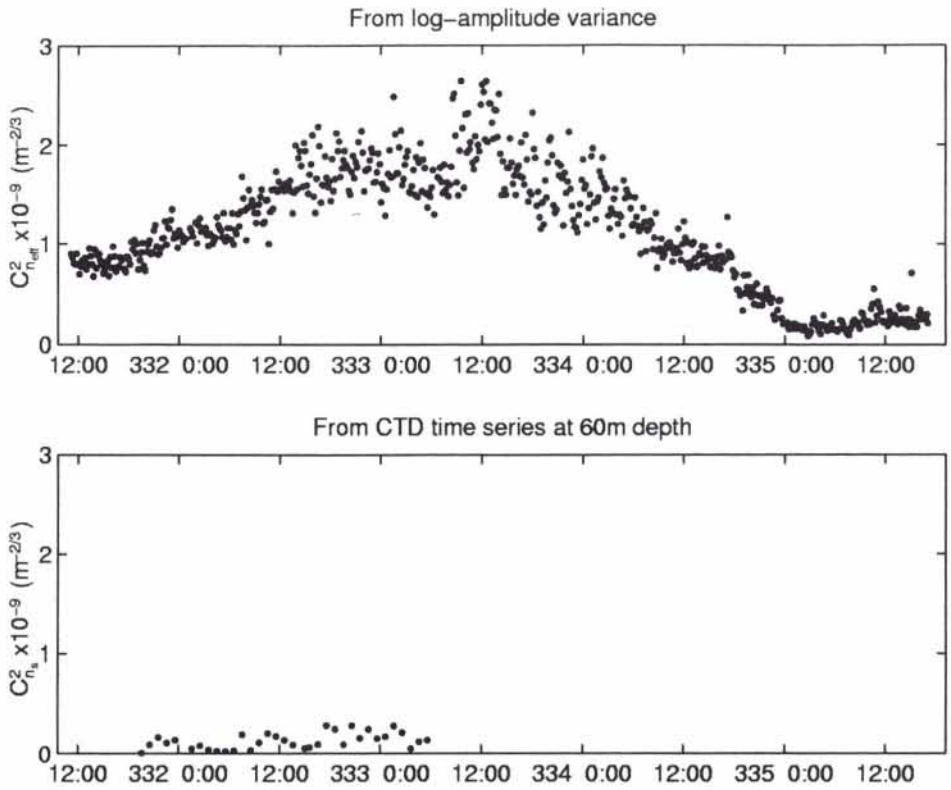

Figure 20 *The level of effective refractive index fluctuations compared with the level of the scalar contribution to the refractive index fluctuations.*

example, the turbulent kinetic energy dissipation rate is determined via,

$$\epsilon^{2/3} = \frac{C^2_{n_v} c_o^2}{1.97}, \tag{5}$$

where c_o is the mean sound speed at the depth of the acoustic path. Acoustic measurements of ϵ range from 1×10^{-6} to 5×10^{-5} $W\ kg^{-1}$. This parameter is useful as it gives the production of turbulent energy caused by shear stresses. Production of energy by buoyancy forces are assumed negligible since the Mediterranean layer is well mixed. Following Monin and Ozmidov (1985) the balance of production and dissipation of energy is then,

$$\frac{\tau_{xz}}{\rho_o}\frac{dU}{dz} + \frac{\tau_{yz}}{\rho_o}\frac{dV}{dz} - \frac{g}{\rho_o} < \rho' w' > = \epsilon, \tag{6}$$

where the shear stresses are given by $\tau_{xz} =< u'w' >$ and $\tau_{yz} =< v'w' >$.

To obtain a first order estimate of the bottom drag coefficient a few assumptions are made. First it is assumed that the measurements are made within a constant

stress layer where $\tau/\rho_o = u_*^2 = C_D U^2$ and the mean shear follows the law of the wall $dU/dz = u_*/\kappa z$ where u_* is the friction velocity, C_D the drag coefficient, $\kappa = 0.4$ is von Karman's constant and z is the distance from the boundary. Neglecting the cross channel flow, Eq. (6) reduces to,

$$\frac{C_D^{3/2} U^3}{\kappa z} = \epsilon. \tag{7}$$

From the path averaged estimates of both U and ϵ 10m from the boundary it is found that the drag coefficient varies from 3×10^{-3} to 15×10^{-3}.

4

Continental Shelf Survey

A basic factor in the study of Black Sea and Mediterranean Sea water exchange is knowing where the dense Mediterranean water finds its way along the shelf toward the slope and the resulting mixing that takes place with the cold intermediate water of the Black Sea. On the shelf, the Mediterranean flow is expected to follow a 'delta' like structure and the salinity dilution is expected to occur quite rapidly compared to mixing within the Strait.

In studying this area the multi-beam SWATH echo sounder was used to obtain detailed bottom bathymetry. CTD profiles were obtained along the canyon and on a 2 mile grid on the shelf in order to locate the Mediterranean effluent and measure the dilution. In addition, a high resolution, high frequency (120 kHz) echo sounder was used for two dimensional imaging of the two layer flow structure.

4.1 SWATH mapping

SWATH mapping was used in order to determine the path of the Mediterranean inflow into the Black Sea, as available bathymetry was not sufficient. The results in Figure 21 show that there is a narrow canyon extending from the Strait of Istanbul (Bosporus). At first the canyon is parallel with the strait and then turns to the northwest where it eventually merges with the continental shelf. A 60 m sill exists within the canyon at its widest point. Mediterranean water is confined and retained within this canyon over a distance of several kilometers until it spreads out on the shelf. Accurate depth measurements are made as simultaneous CTD profiles, from which sound speed is calculated, were obtained along the path of the underwater canyon.

4.2 CTD profiles

A series of CTD profiles from NRV *Alliance* were taken within the canyon, where Mediterranean inflow was confined to the bottom. The stations are shown in Figure 22(a) which spans a 36 h period from Julian day 330 to 331. Once the detailed bottom bathymetry was obtained, TCG *Çubuklu* was able to follow the canyon

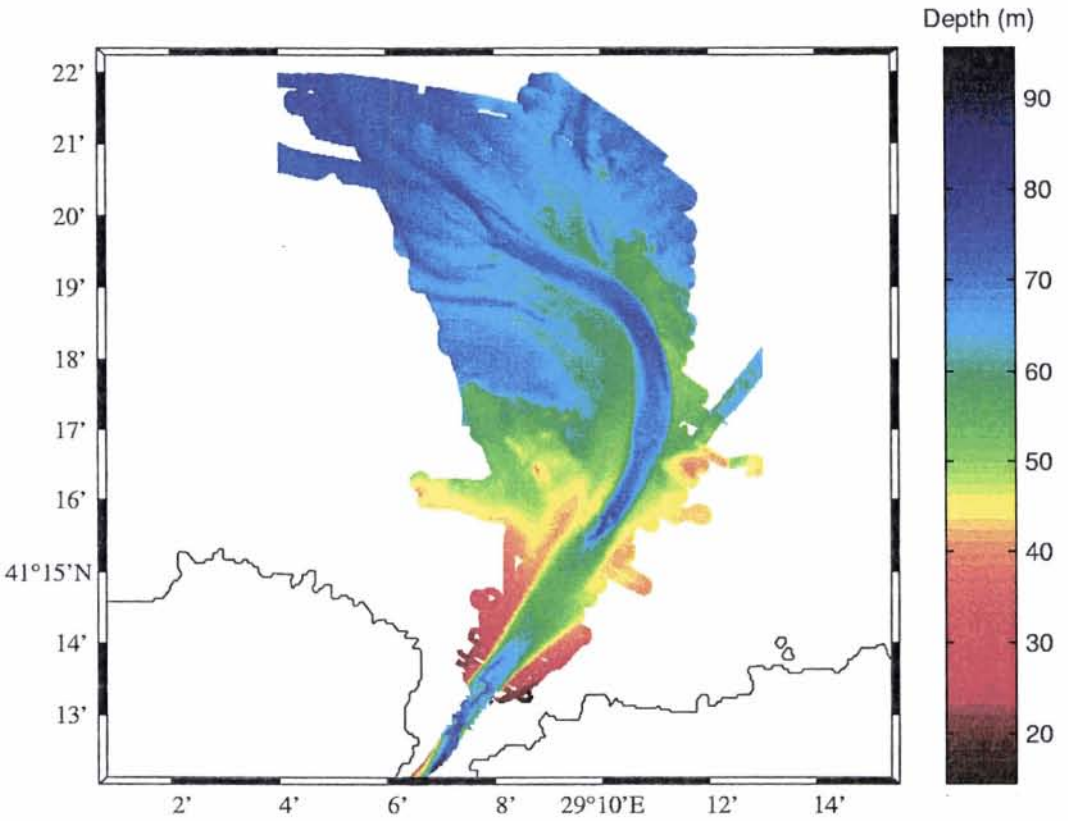

Figure 21 *Bottom bathymetry in the Black Sea exit region using the multi beam SWATH echo sounder.*

collecting CTD profiles as shown in Figure 22(a) over a 5 h period on Julian Day 333. In addition, a two-mile grid of CTD profiles was obtained from NRV *Alliance* and TCG *Çubuklu* in order to cover the shelf and part of the slope area (see Figure 22(b)). During good weather conditions it was possible to sample the water column close to the bottom in order to determine Mediterranean water characteristics. With these measurements the highly saline water was traced over several kilometers and its dilution with overlying Black Sea water observed.

Figures 23(a) and (b) show the temperature and salinity variations along the canyon. The range is calculated from the southernmost CTD station in Figure 22(a) so that the bathymetry remains approximately the same for each transect. The images depict Mediterranean flow over the sill. Measurements show that the dense water enters the Black Sea with a salinity of 36 psu. According to Ünlüata et al. (1990) the Mediterranean enters the Strait of Istanbul (Bosporus) from the Marmara Sea with salinity 37 psu. Thus, during its passage of 35 km through the Strait, only 1 psu is diluted with the Black Sea water. As the Mediterranean makes its way along

(a)

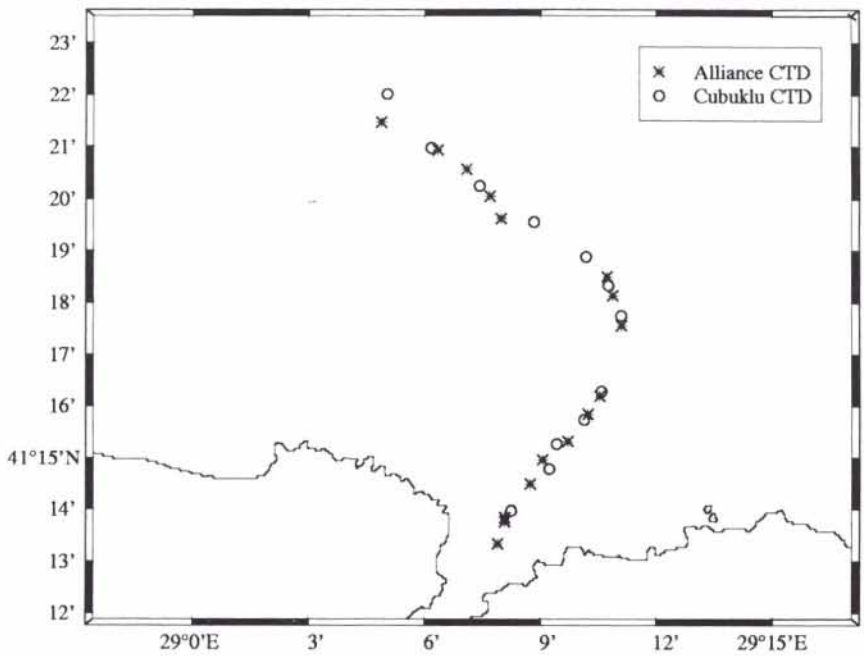

(b)

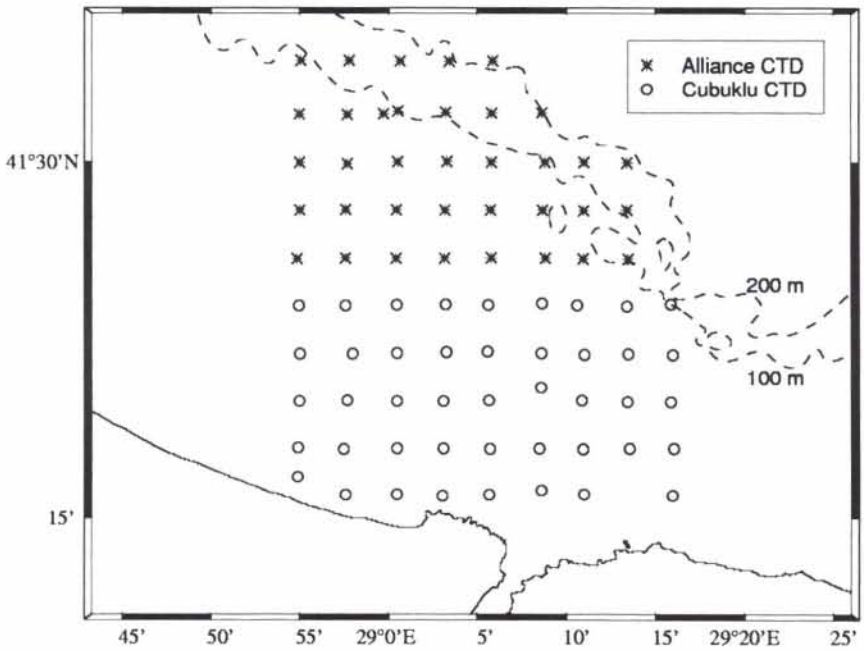

Figure 22 *CTD stations by NRV Alliance and TCG Çubuklu (a) along the canyon and (b) taken on a two mile grid.*

the canyon of the Black Sea, the effluent is diluted to 33 psu. A further reduction of 3 psu over a 20 km transect. Thus the dilution is expected to continue quite rapidly on the shelf until it finally reaches the continental slope.

The images of temperature in Figures 23(a) and (b) also show the presence of cold intermediate Black Sea water. There is a 2 day difference between the measurements and on Julian Day 333, when the Mediterranean outflow was at its maximum, the cold intermediate water has made its way south toward the sill.

The temperature and salinity data from the grid stations in Figure 22(b) are shown in Figures 24(a) and (b) respectively. The northernmost and southernmost horizontal transects are shown at the top and bottom of the page respectively. The + indicates 10°C for the temperature profiles and 22 psu for the salinity. The temperature profiles show substantial spatial variability because of mixing between the warm surface waters and the cold intermediate water. The salinity profiles can be used to track the Mediterranean inflow and measure the dilution. These profiles give a characteristic temperature-salinity relation for the Black Sea. The results are shown in Figure 25 with contours of σ_t. The cold intermediate water of the Black Sea on the continental shelf occurs between depths 50 - 75 m (Özsoy et al., 1993) is a permanent feature of the Black Sea. The vertical spread in the interface region is a result of the mixing between Mediterranean Sea water and the cold intermediate water on the shelf.

Figure 26 shows the location of bottom salinity values greater than 24 psu which indicates the presence of Mediterranean water; deep Black Sea water is 22.3 psu beyond 1000 m depth. On the shelf, the Mediterranean water spreads to a few metres thick and it is possible that some of the CTD profiles did not reach the layer. Nevertheless, the extent of the spreading and the path of the Mediterranean inflow can be seen. The salinity values documented here, differ from those documented by Latif et al. (1991). At the 100 m contour they observed salinities ranging between 20 and 22 psu. Our measurements show salinities of 25 and 30 psu close to the 100 m contour. These high salinity values imply the formation of a water mass dense enough to sink to and hence cause renewal of, the deep Black Sea water.

4.3 Echo sounding images

The presence of Mediterranean water is inferred using a high resolution, high frequency (120 kHz) echo sounder (on loan from the Institute of Ocean Sciences, Canada) towed alongside either NRV *Alliance* or TCG *Çubuklu*. Figure 27 shows sample survey lines taken on the shelf where two dimensional imaging of the Mediterranean flow are observed. Knowing the bathymetry, it was possible to make a transect along the canyon and then continue along the shelf where Mediterranean water was expected to flow. A number of cross sections along the canyon were also

(a)

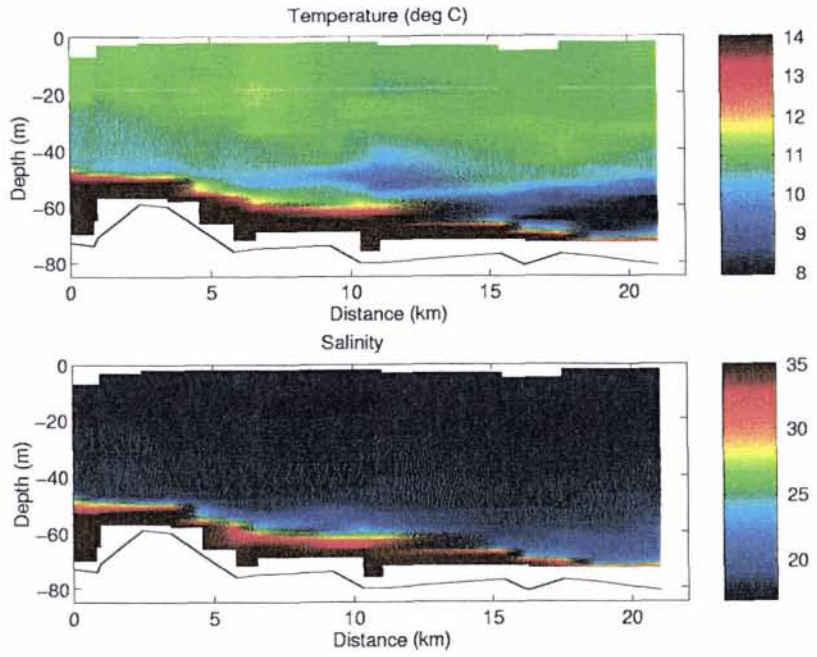

(b)

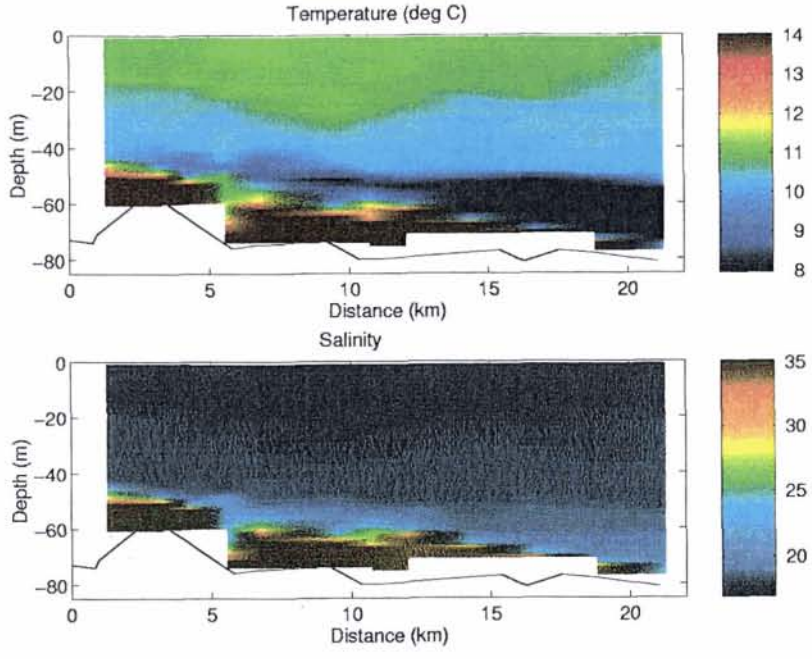

Figure 23 *Temperature and salinity taken along the canyon from (a) NRV Alliance on Julian Day 330/331 and (b) TCG Çubuklu on Julian Day 333.*

(a)

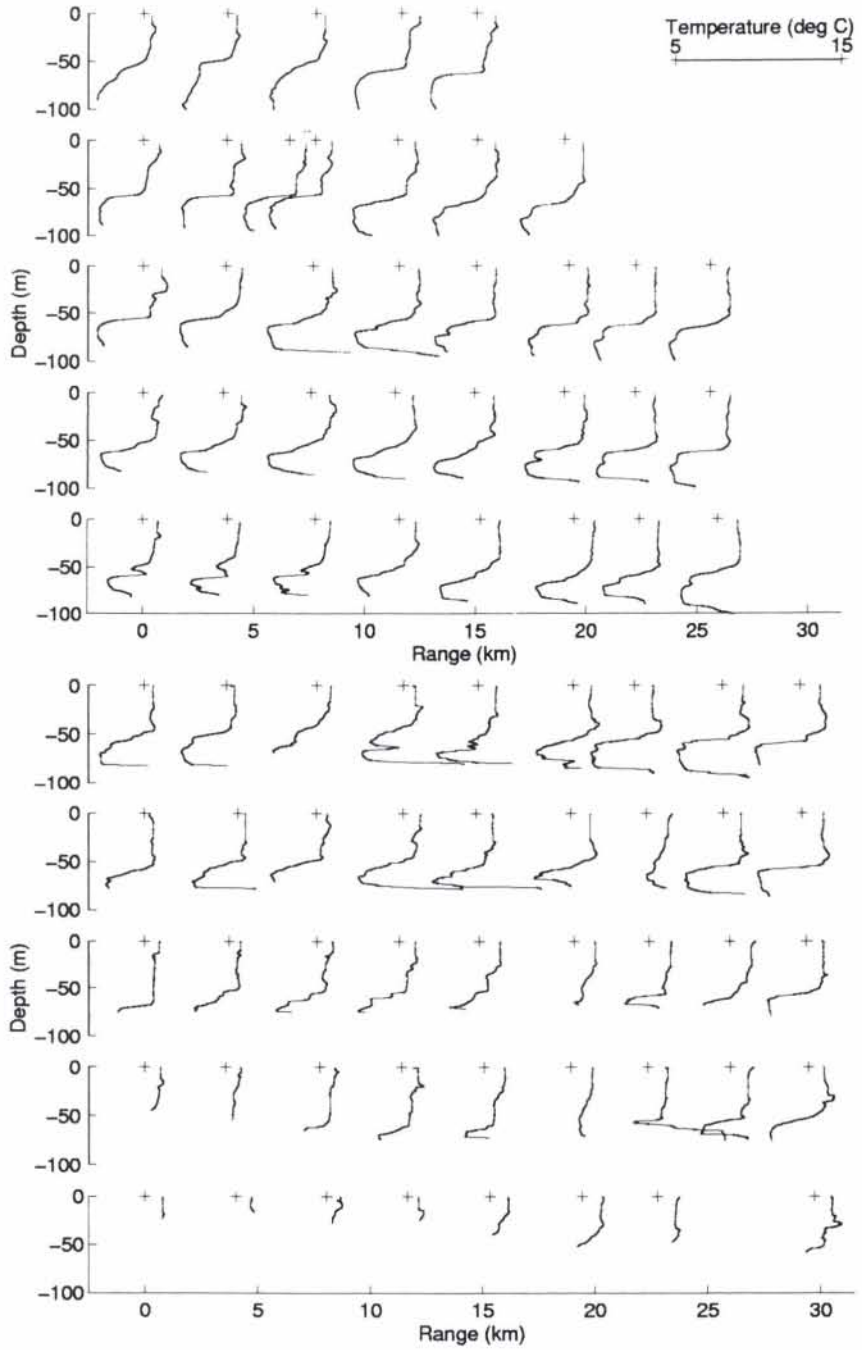

Figure 24 *(a) Temperature (+ = 10°C) and (b) salinity (+ = 22) profiles obtained on a two mile grid.*

(b)

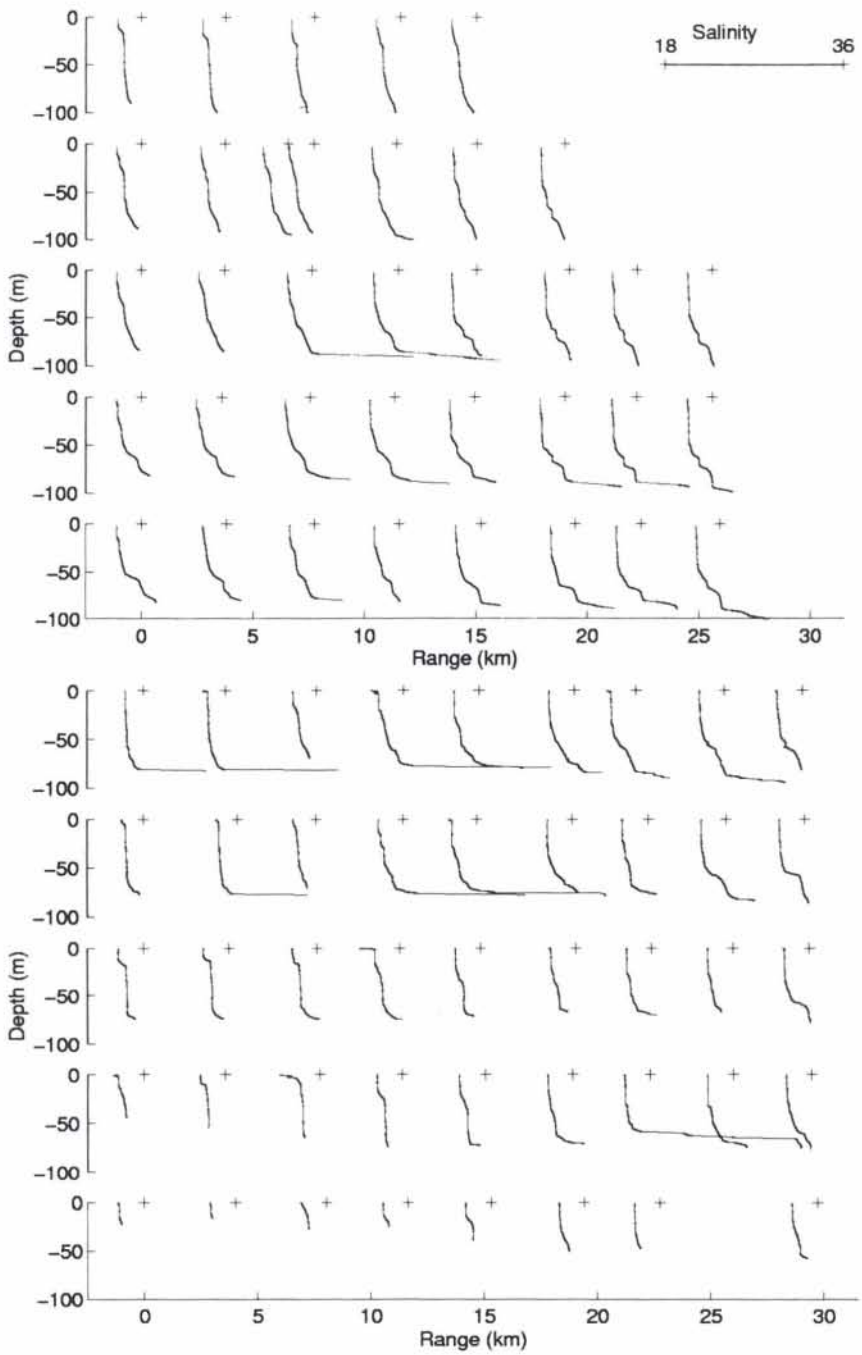

Figure 24 continued.

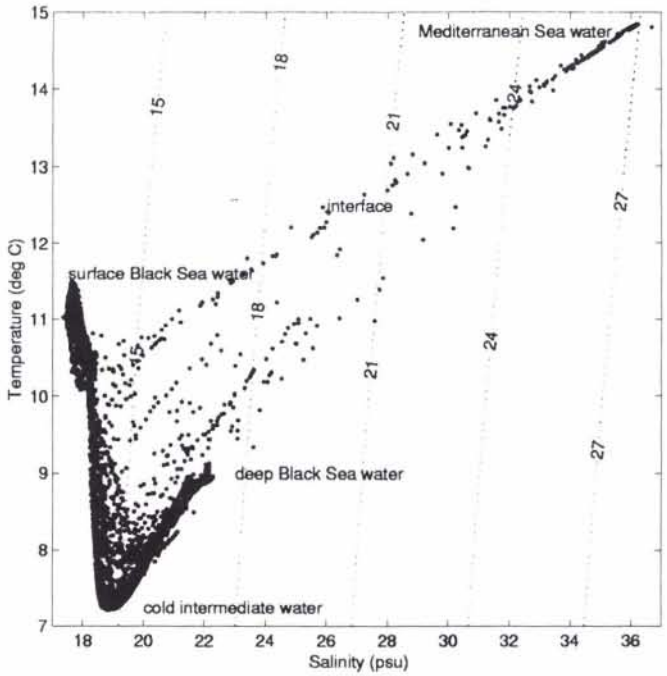

Figure 25 *Temperature-salinity diagram for profiles taken on the continental shelf and slope.*

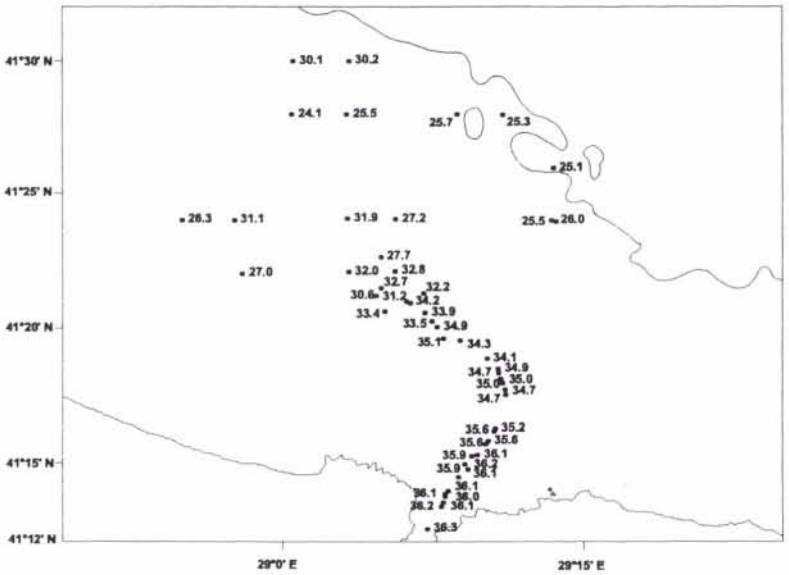

Figure 26 *Bottom salinity values greater than 24 psu.*

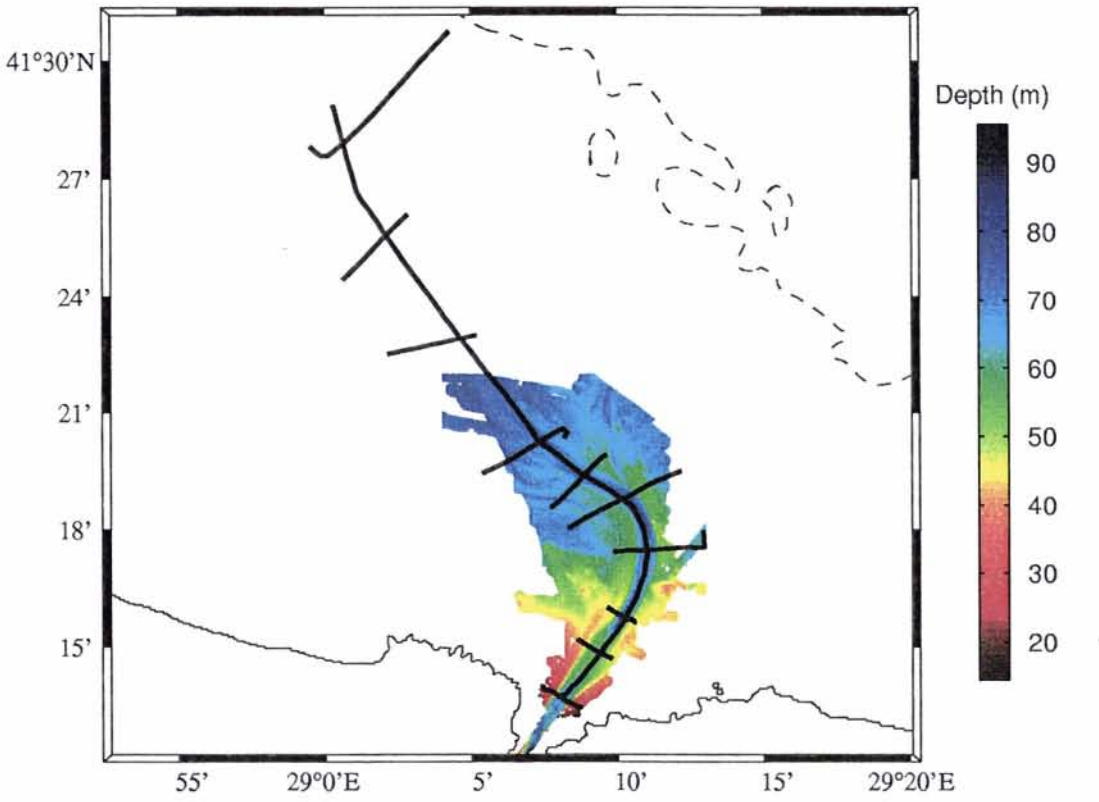

Figure 27 *Transects along and across the canyon where high resolution echo sounding images were obtained.*

made, in order to observe the spreading of Mediterranean water on the shelf. The 100 m contour line shown in Figure 27 indicates approximately the start of the continental slope.

The acoustic characteristics and operating parameters for the Biosonics echo sounder are shown in Table 4. The narrow beamwidth, the small pulse length and fast transmission rate allow high resolution measurements of the two layer structure. Sound is scattered by small fish, zooplankton and temperature microstructure.

Figure 28 shows a 35 km transect along the canyon from South to North with temperature profiles from expendable thermistors (XBTs) superimposed. The images have been heavily subsampled (time interval $\sim 2s$) so that the 35 km transect can be viewed. The survey was conducted on Julian day 348 when the Mediterranean inflow was strong as was seen with ADCP data in Figure 3. As the depth of the echo sounding images is calculated on the basis of a mean sound speed profile, errors in the depth can be ± 2 m and this may explain why there is a vertical offset between some of the XBT profiles and the echo of the pycnocline.

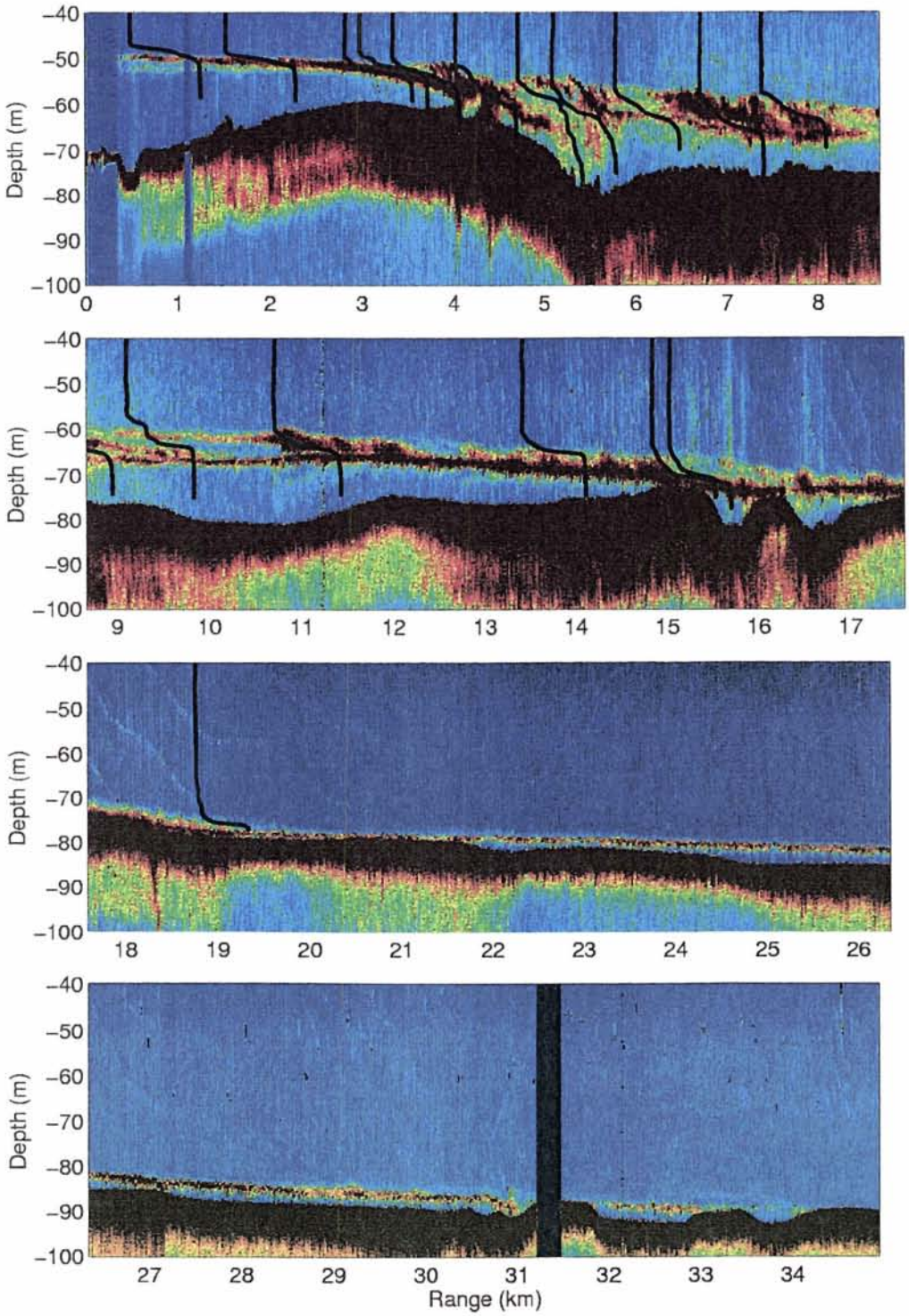

Figure 28 *Acoustic back scatter images taken over a 35 km transect along the canyon and continental slope.*

Parameter	quantity
Source level	215.3 dB re $1\mu Pa$ @ $1m$
Beam width	3.8 degrees
Pulse width	0.2 ms
Transmission interval	0.2 and sometimes 0.3 s
Time variable gain	$20 \log r$

Table 4 *Echo sounding instrument parameters.*

Biological matter distributed at the interface together with temperature microstructure contributes to the acoustic back scatter characteristics as discussed by Farmer and Denton (1985) for their images of flow over a sill. Strong back scatter from the interface is observed. Measurements show that the normal incidence echo level from the interface is 40% that of the bottom reflection. Strong spatial variations in the acoustic backscatter are visible at the interface which is presumably associated with turbulent mixing along the canyon.

The sill at 60 m depth is located 3 km from the entrance to the Strait of Istanbul (Bosporus). According to the model results of Oğuz et al. (1990) the hydraulic control for Mediterranean flow into the Black Sea occurs 1 km downstream of the sill crest and that supercritical flow encompasses a distance of 1 km North of the control section.

North of the sill, the density current plunges down the sill slope causing the Mediterranean layer to become turbulent. Measurements from a 1996 sea trial showed current speeds exceeding 1 $m\ s^{-1}$ in this area. Further North, the Mediterranean layer restratifies into a well mixed layer as is apparent from the temperature profiles. As the Mediterranean water flows onto the shelf it becomes very thin as a result of spreading as bathymetric control disappears into a delta. The dilution of the effluent as seen by Figure 26 occurs quite rapidly beyond the sill because the layer decreases to a few metres.

Echo sounding cross sections along the canyon at locations [0.1 3.2 5.2 8.7 11.3 13.7 16.3 22.5 28.4 33.5] km in Figure 28 are shown in Figure 29. The cross sections were taken on Julian days 333, 330, 331, 333, 333, 348, 348, 348, 348, 348 respectively and thus correspond to when the Mediterranean inflow was strong as was seen from ADCP data in Figure 3. The depth range covers 60 m and is to scale from image to image but the horizontal distances are not to scale and vary. Ten images are shown corresponding to the southernmost transect first and the northernmost transect last of Figure 27. The range is set so that 0 km corresponds to the location where the along canyon transect was taken; negative (positive) range values thus correspond to the distance left (right) of the along canyon transect.

The first image of Figure 29 is a cross section South of the sill where the ADCP and

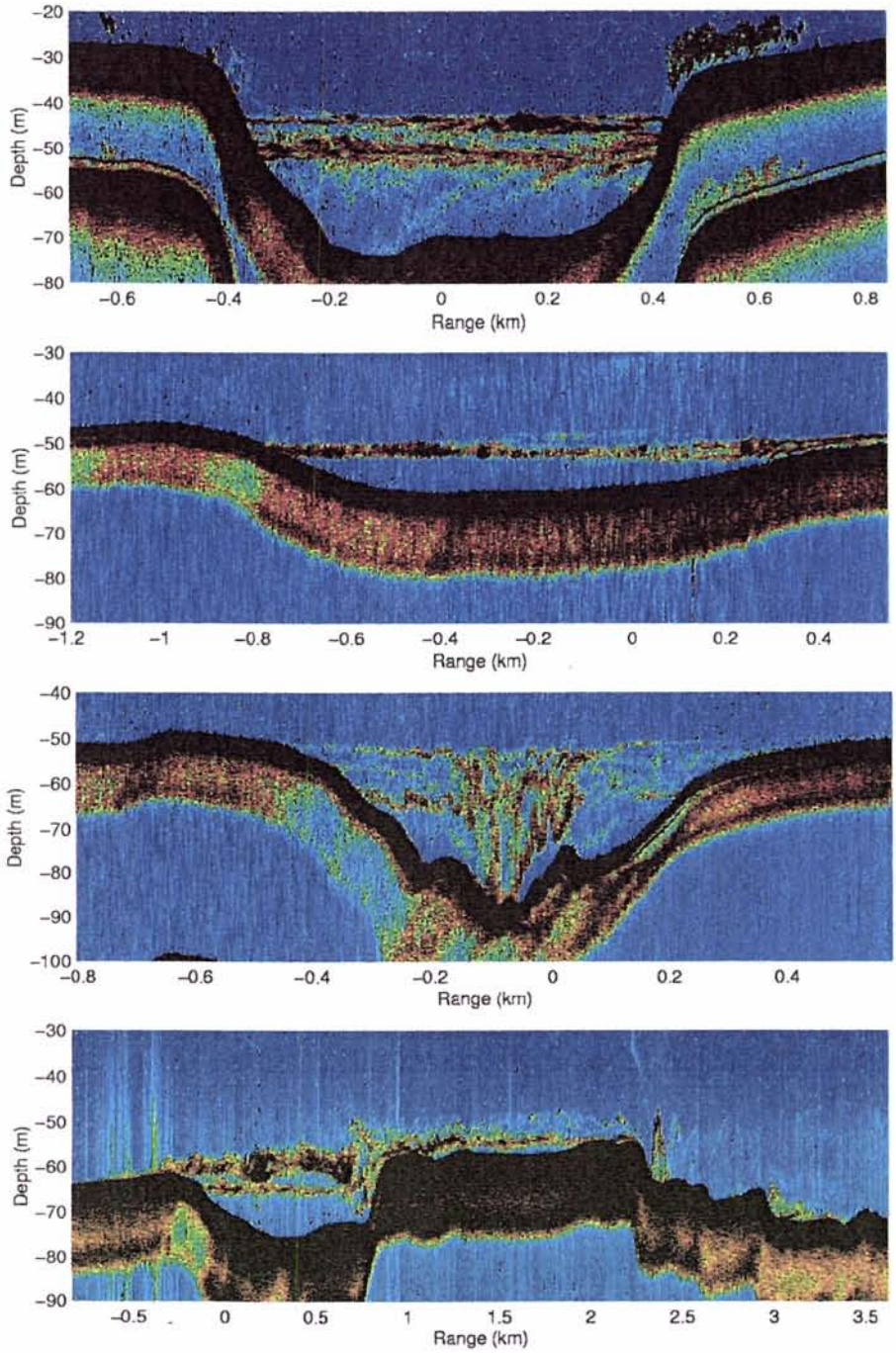

Figure 29 *Acoustic back scatter images taken across the canyon. Images are shown from southernmost cross section to northernmost and are located at [0.1, 3.2, 5.2, 8.7, 11.3, 13.7, 16.3, 22.5, 28.4, 33.5 km] in Figure 28.*

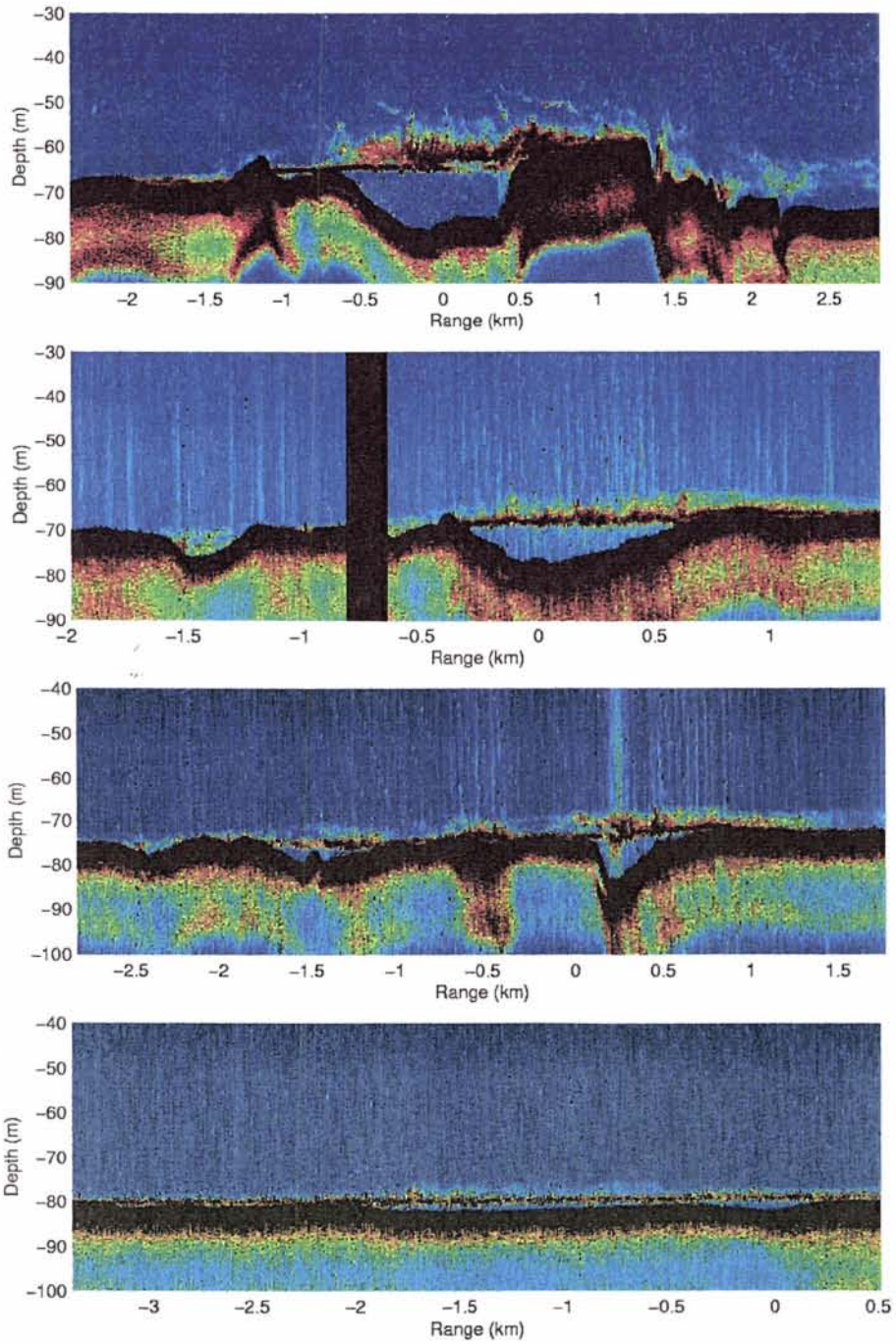

Figure 29 continued

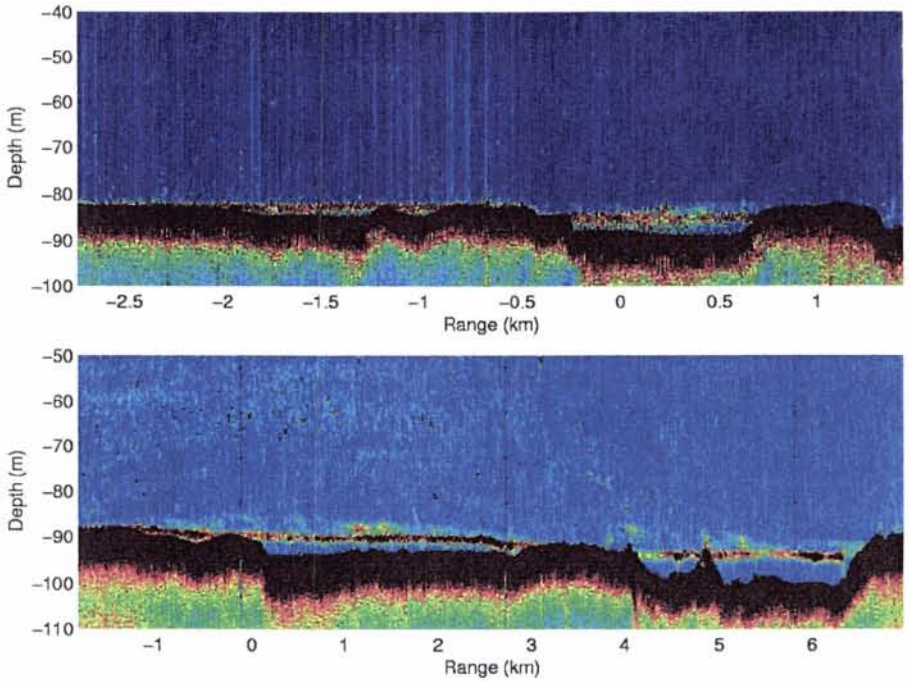

Figure 29 continued

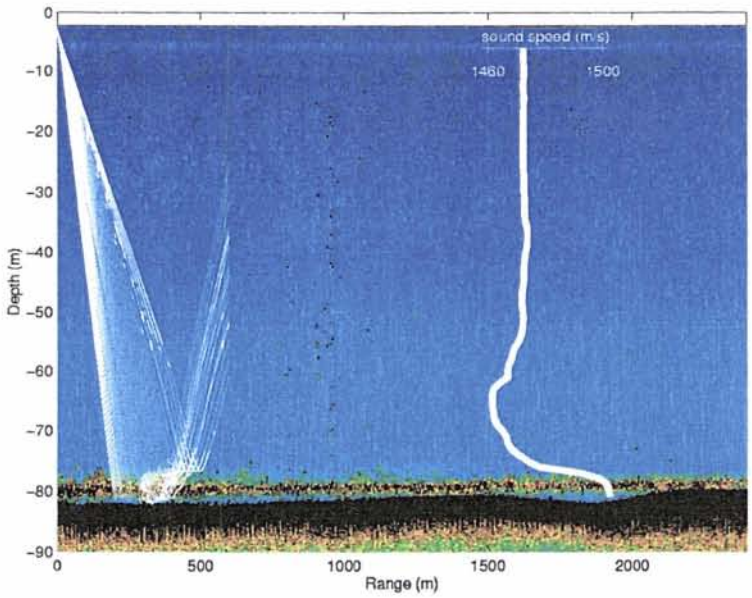

Figure 30 *Echo sounding image with superimposed sound speed profile. The rays from a forward looking sonar are also superimposed.*

acoustic scintillation instruments were moored and where the flow is subcritical. To the east of the canyon, the acoustic echoes show a school of fish. The second image is taken across the sill. The third image is taken $\sim$ 2 km North of the sill which according to the model results of Oğuz et al. (1990) is just within the super critical regime.

The fourth and fifth images are taken at the point where the canyon turns to the northwest. Because of channel curvature there may be a cross channel circulation that causes Mediterranean water to accumulate on the right, thus spilling over the canyon edge. As the flow enters the bend, it is hypothesized that the interfacial waters move to the outside of the bend and salty warm water from below is brought to the interface on the inside of the bend. This flow structure within the Mediterranean layer could cause vertical mixing because of instability and needs to be confirmed by observation. According to Oğuz et al. (1991) the regional circulation of the Black Sea exit region follows the topography and divides into two parts outside the Strait of Istanbul (Bosporus). The first continues toward the east and is incorporated with the general circulation of the Black Sea. The second is deflected towards the South and enters the Strait of Istanbul (Bosporus). This circulation pattern could also displace water from the canyon during times when Mediterranean water inflow is at a maximum.

Spreading of the Mediterranean effluent has filled adjacent canyons to the left of the main canyon as seen by the fifth, sixth and seventh image. As the canyons merge with the shelf, the Mediterranean effluent spreads horizontally as seen by the eighth image. Finally the last two images correspond to cross sections taken just prior to the continental slope. These images show the presence of two main shallow canyons filled with the effluent. This implies that there could be a major canyon to the right of the eighth and ninth image which we did not survey. This canyon would correspond to the right most canyon of the tenth image.

The effect of the Mediterranean sea layer close to the bottom on forward looking sonars can be seen in Figure 30. Superimposed on the echo sounding image is a profile of sound speed. With this sound speed profile, ray traces from a forward looking sonar looking outward from 200 to 500 m show that half the energy is reflected from the interface. These rays never touch the sea floor. Measurements show that the critical angle is approximately 75^o from the vertical ($\theta_c = \arcsin(c_B/c_M)$). Rays projected at angles less than this will touch bottom and those at angles greater will be reflected from the Mediterranean sea layer. This environment makes it difficult to detect objects on the sea floor.

5

Large Scale Survey

Beyond the shelf, the diluted Mediterranean water sinks down the continental slope to a depth appropriate to its density and is then incorporated in the eastward general circulation of the Black Sea. It is expected to be found as occasional intrusions differing in temperature and salinity to the surrounding water. With this in mind a large scale survey was carried out. This survey consists of NOAA satellite images of sea surface temperatures and current measurements from the 75 kHz ADCP system on board NRV *Alliance*.

Parameter	quantity
Survey 1	28-NOV-1995 09:02 to 29-NOV-1995 04:56 UTC
Survey 2	30-NOV-1995 09:07 to 02-DEC-1995 05:57 UTC
Frequency	75 kHz
Transmission rate	0.5 Hz
Ensemble average	60 transmissions
Ensemble interval	5 min
Bin length	8 m
Total Bins	16
Depth range	18 to 146 m

Table 5 *Ship mounted ADCP instrument parameters.*

5.1 Ship mounted ADCP

The large-scale general circulation of the southwestern Black Sea is studied using the 75 kHz ADCP on board NRV *Alliance*. Table 5 lists the set up parameters and measurement time for this system. Figure 31 shows the ship track and Figure 32 the current vectors. The flow from the northwestern Black Sea basin mainly follows the topography. At the exit region the flow divides into two parts, one of which continues toward the east, the other interacting with the Strait of Istanbul (Bosporus) canyon. This interaction causes the current to deflect toward the South and enter partially

into the Strait of Istanbul (Bosporus). This southerly flow creates an anticyclonic flow along the northwest coast as observed in Figure 32(a). Figure 32(b) shows the current vectors over a larger space and time scale. When the winds change from southerly to northerly much variability in the current structure can exist during this larger scale survey time.

5.2 Sea surface temperatures

The sea surface temperatures during times at which there was no or little cloud cover are shown in Figure 33. These satellite images can be useful to outline specific oceanographic features namely anticyclonic or cyclonic eddies and oceanographic fronts. For example on Nov 27/28 an anticyclonic eddy is presumably featured at the Black Sea / Strait of Istanbul (Bosporus) region. Much variability is shown between the November and December images. This can be assumed to be the result of strong changes in meteorological conditions.

(a)

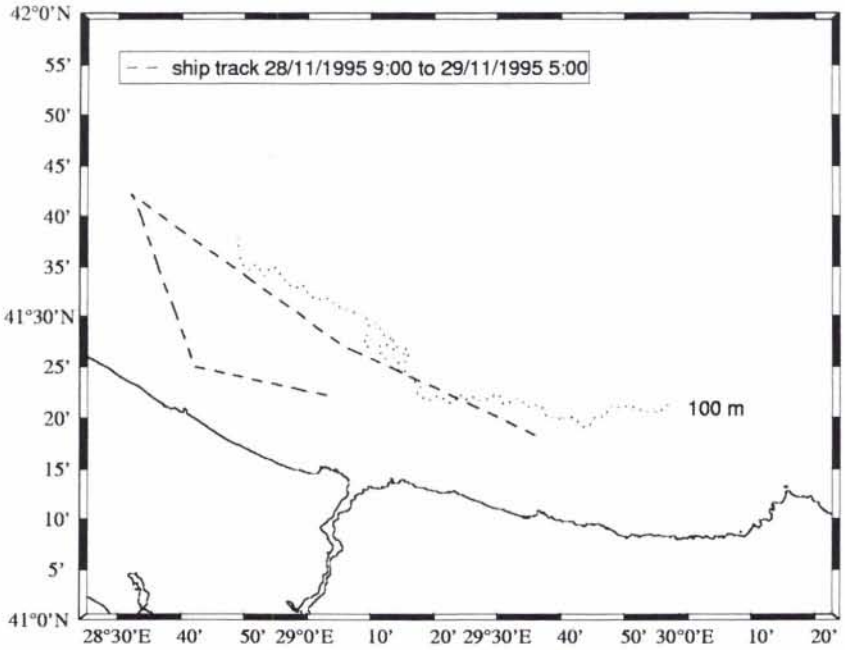

(b)

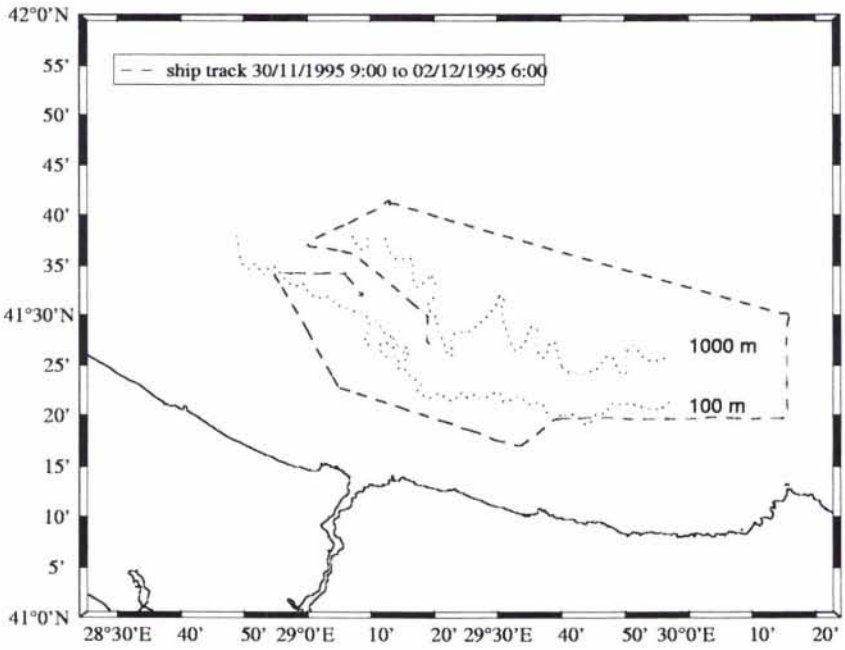

Figure 31 *Ship track for ADCP measurements during (a) Nov 28-29, 1995 and (b) Nov 30 - Dec 02, 1995.*

(a)

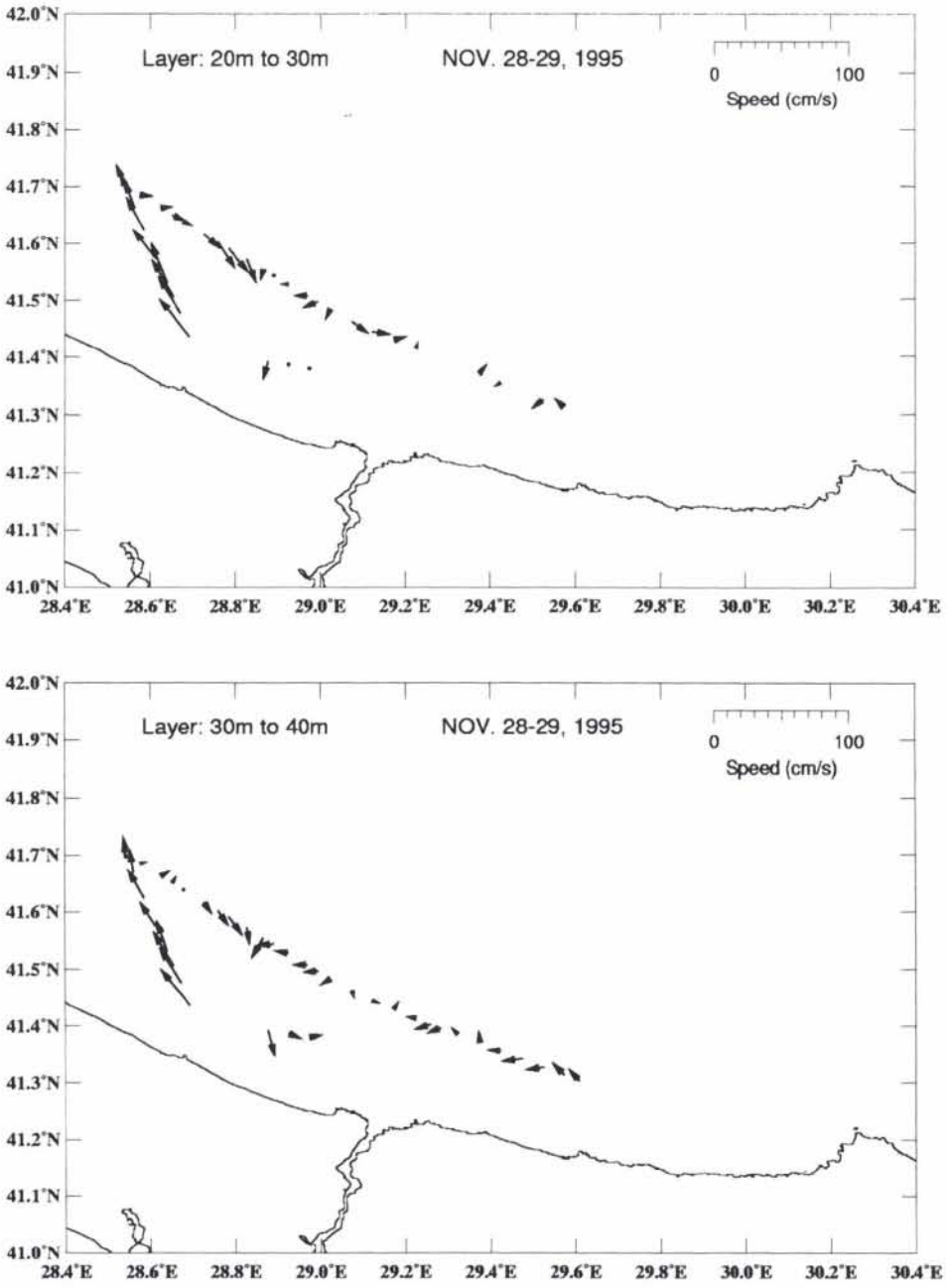

Figure 32 *Current vectors as a function of depth obtained from the ship mounted ADCP during (a) Nov 28-29, 1995 and (b) Nov 30 - Dec 02, 1995.*

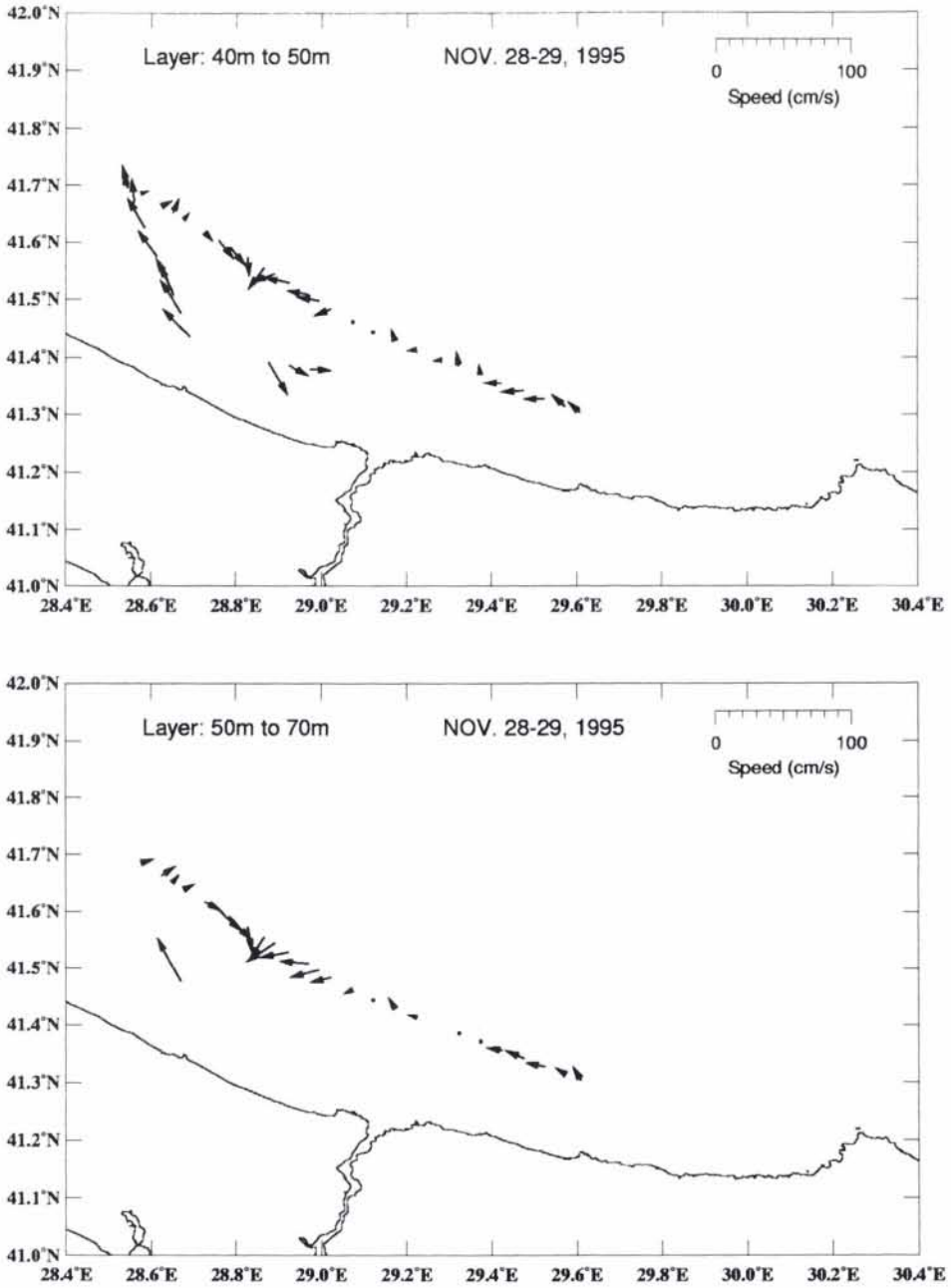

Figure 32 continued.

(b)

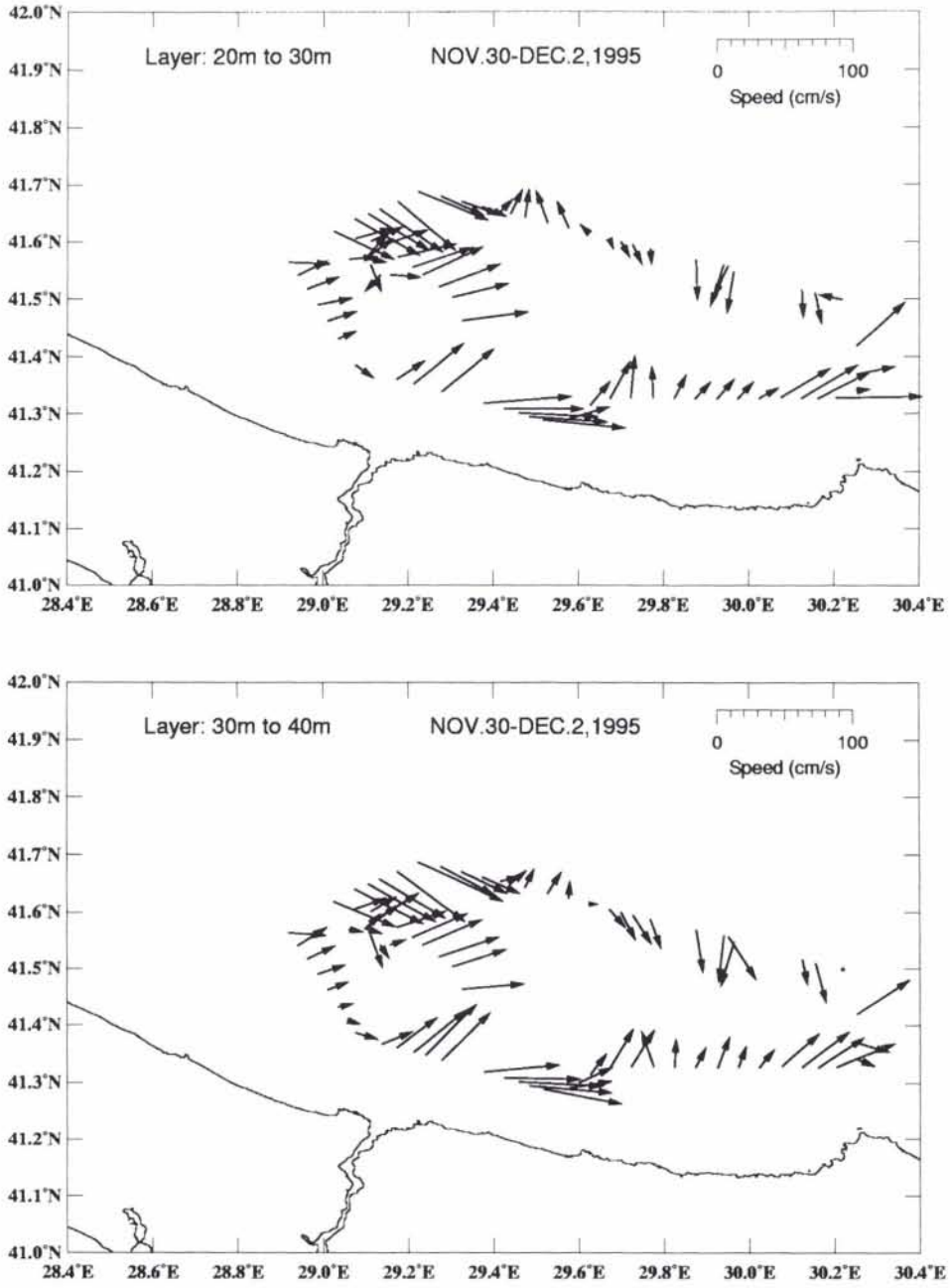

Figure 32 continued.

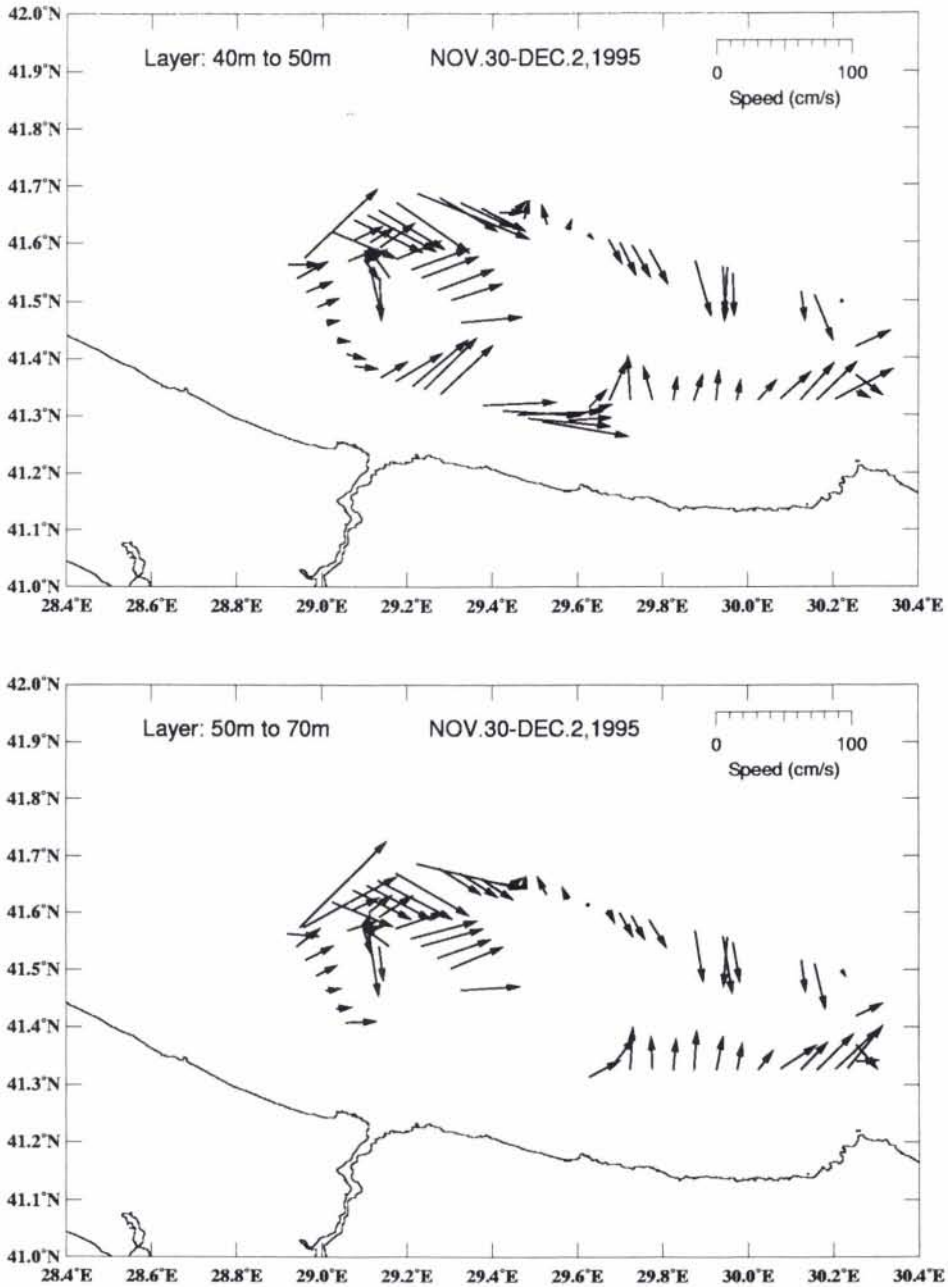

Figure 32 continued.

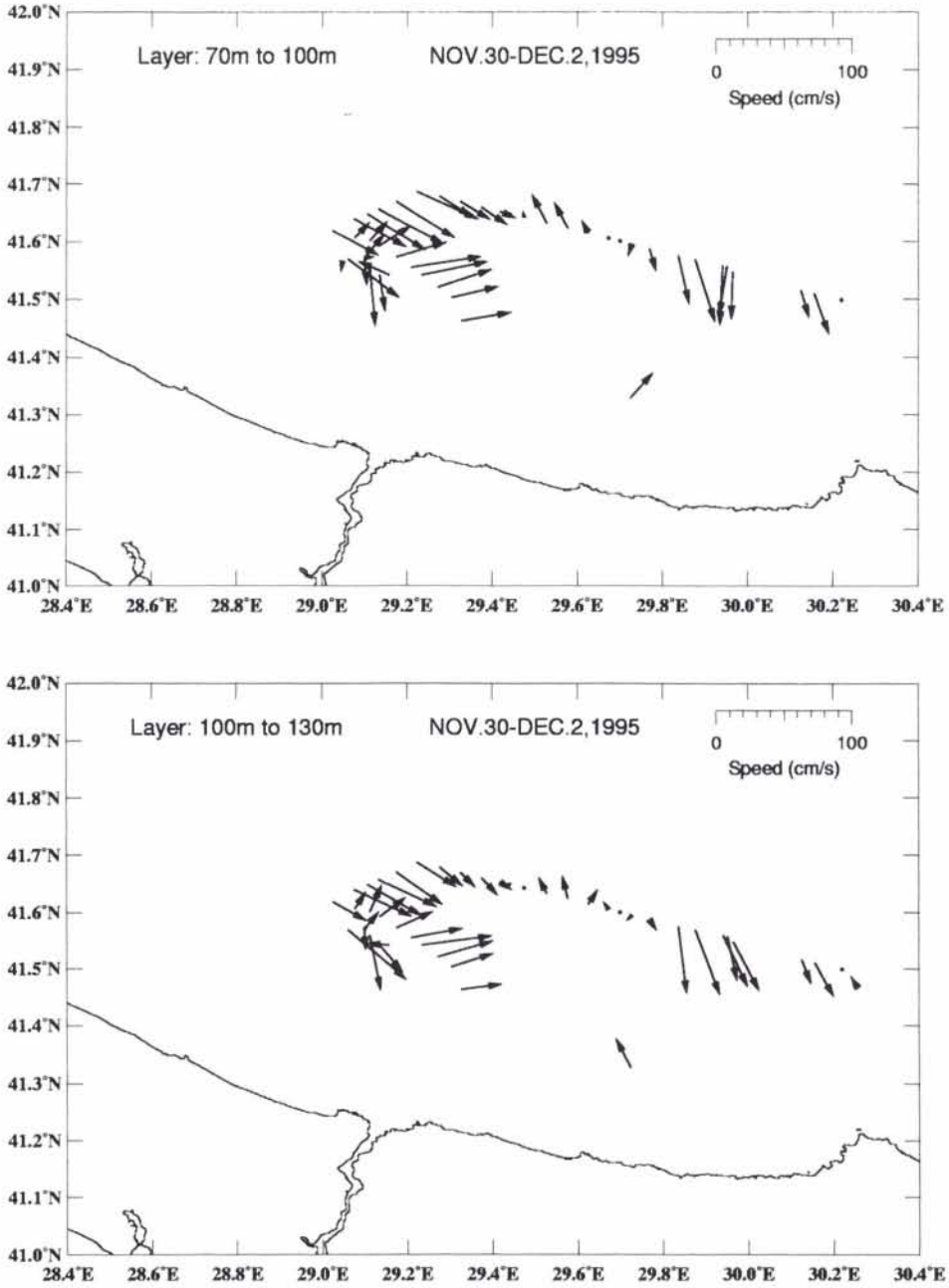

Figure 32 continued.

(a)

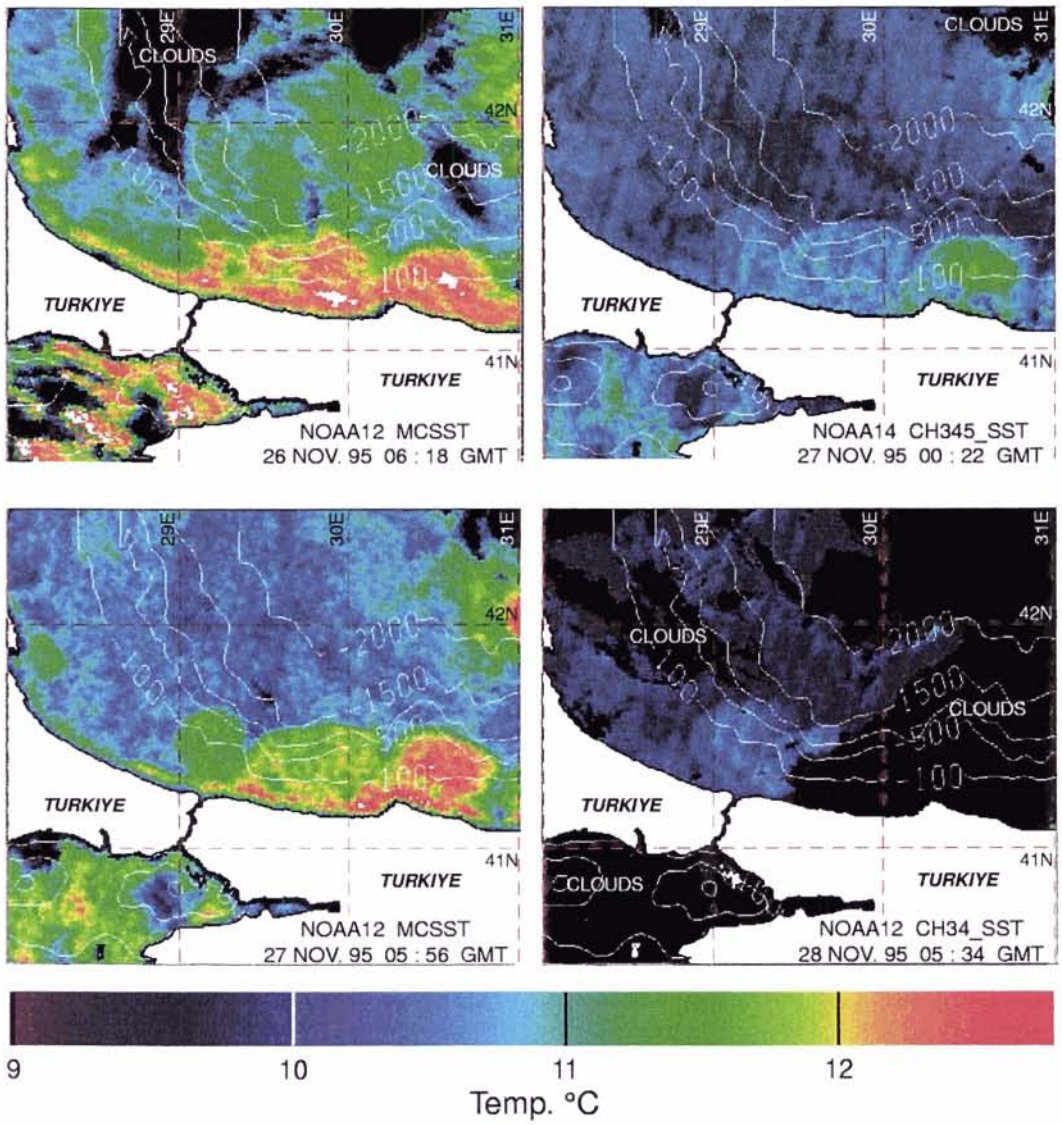

Figure 33 *Sea surface temperatures from NOAA satellite for (a) November 1995 and (b) December 1995.*

(b)

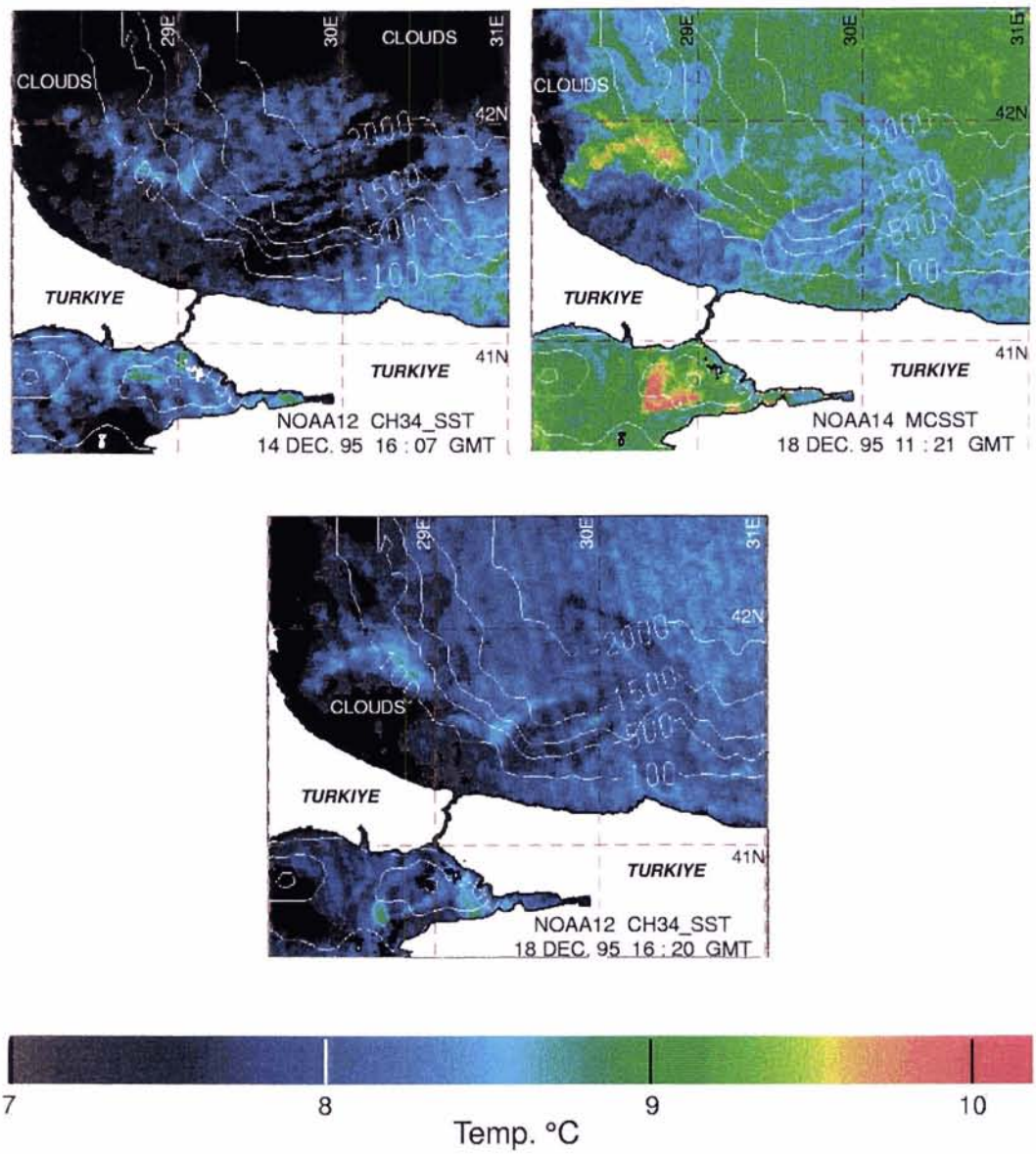

Figure 33 continued.

6

Conclusion

This report summarizes the variety of acoustic and oceanographic data collected during the 1995 sea trial in the Black Sea. Significant spatial and temporal variability was observed in the Mediterranean flow into the Black Sea. For example, the moored ADCP measurements showed temporary but complete blockage of the Mediterranean undercurrent. This blockage was shown to correspond to times when the relative sea level difference was greater than 45 cm. The ADCP measurements also showed that the Mediterranean undercurrent exhibits Ekman spiral currents because of bottom and interfacial friction.

Profiles and time series of temperature and salinity at a fixed location showed a high degree of mixing between the Black Sea and Mediterranean water. This mixing was observed by the increase in salt content of the Black Sea layer. The CTD and current velocity profiles give a measure of shear instability parameterized by the Richardson number. It was found that over the 36 h measurement period when the Mediterranean undercurrent was strong, the flow was consistently turbulent, due to shear instabilities in the depth range 50 - 60 m.

The turbulent levels within the Mediterranean boundary layer were observed using an acoustic scintillation instrument. Analysis of the acoustic amplitude showed increased variability with increasing current strength. Given that the contribution of temperature and salinity variations to the total acoustic scattering was found to be negligible is was concluded that turbulent velocity variations dominated the acoustic scattering.

SWATH mapping showed that the Mediterranean flow is confined within a well defined canyon which initially is oriented in the northeast direction and then turns toward the northwest. During the SWATH mapping, simultaneous CTD profiles were obtained in order to measure the dilution of the Mediterranean effluent. In addition, a two mile grid of CTD profiles from NRV *Alliance* and TCG *Çubuklu* showed bottom salinity values of 30.3 psu very close to the continental slope indicating that the dilution was at most 6 psu.

High resolution echo soundings gave two dimensional imaging of the two layer flow. As the mixing between the two very different water masses is turbulent, a strong acoustic back scatter is obtained, revealing detailed, interfacial structure. The Med-

iterranean effluent was traced along the canyon and the shelf. Observations show that on the shelf the Mediterranean flow exhibits a 'delta' like structure. Although flow is controlled by topography, spillage over the canyon is observed. Mediterranean water spreads over a larger area compared with previous findings (Latif et al., 1991). This thin layer of dense water masks the effects of the sea bottom (100 m depth) on acoustic propagation for shallow angles (critical angle, $\theta_c = 75^o$).

The large scale ADCP survey shows the general eastward circulation pattern of the southwestern Black Sea region. Sea surface temperatures from NOAA satellites show a high degree of variability during the experimental period.

7 Acknowledgements

The authors wish to thank the officers and crew of the NRV *Alliance*, TCG *Çubuklu* and the Turkish Navy Department of Navigation, Hydrography and Oceanography for their assistance in the collection of acoustic and oceanographic data. Many thanks to R. Della Maggiora and A. Brogini for their efforts in preparing the oceanographic instrumentation and G. Baldasserini for carrying out the preliminary oceanographic data processing. The swath processing was carried out by A. Trangeled and C. Sisti. NOAA satellite images were prepared by E. Nacini.

References

Di Iorio, D. and Farmer, D. (1998). Separation of current and sound speed in the effective refractive index for a turbulent environment using reciprocal acoustic transmission. *Journal of the Acoustical Society of America*, 103:321–329.

Farmer, D. and Denton, R. (1985). Hydraulic control of flow over the sill in Observatory Inlet. *Journal of Geophysical Research*, 90:9051–9068.

Latif, M., Özsoy, E., Oğuz, T., and Ünlüata, U. (1991). Observations of the Mediterranean inflow into the Black Sea. *Deep-Sea Research*, 38:S711–S723.

Monin, A. and Ozmidov, R. (1985). *Turbulence in the Ocean.* Reidel.

Oğuz, T., Özsoy, E., Latif, M., Sur, H., and Ünlüata, U. (1990). Modeling of hydraulically controlled exchange flow in the Bosphorus Strait. *Journal of Physical Oceanography*, 20:945–965.

Oğuz, T., Latif, M., Sur, H., Özsoy, E., and Ünlüata, U. (1991). On the dynamics of the southern Black Sea. In Izdar, E. and Murray, J., editors, *Black Sea Oceanography, NATO-ASI Series.* Kluwer Academic Publishers, the Netherlands.

Özsoy, E., Ünlüata, U., and Top, Z. (1993). The evolution of Mediterranean water in the Black Sea: interior mixing and material transport by double diffusive intrusions. *Progress in Oceanography*, 31:275–320.

Tatarskii, V. (1971). *The Effects of the Turbulent Atmosphere on Wave Propagation.* Translated from Russian by Israel Program for Scientific Translations, Jerusalem.

Tolmazin, D. (1985). Changing coastal oceanography of the Black Sea. II: Mediterranean effluent. *Progress in Oceanography*, 15:277–316.

Ünlüata, U., Oğuz, T., Latif, M., and Özsoy, E. (1990). On the physical oceanography of the Turkish Straits. In Pratt, L., editor, *The Physical Oceanography of Sea Straits.* Dordrecht, the Netherlands, Kluwer.

Yüce, H. (1996). Mediterranean water in the Strait of Istanbul (Bosphorus) and the Black Sea exit. *Estuarine, Coastal and Shelf Science*, 43:597–616.

Report no. changed (Mar 2006): SR-294-UU

Document Data Sheet

Security Classification		Project No.
		022-1
Document Serial No.	**Date of Issue**	**Total Pages**
SR-294	June 1998	66 pp.

Author(s)

Di Iorio, D., Akal, T., Sellschopp, J., Guerrini, P., Yüce, H., Gezgin, E.

Title

Oceanographic measurements of the West Black Sea: November 26 to December 14, 1995.

Abstract

Mediterranean water inflow into the Black Sea is investigated using acoustic and oceanographic data obtained in the Black Sea exit region. Temporal and spatial variability in the flow and their relation to atmospheric and sea level changes are documented. The turbulent boundary layer formed by Mediterranean flow over the sea bottom results in turbulent mixing because of hydrodynamic instability. The path of Mediterranean Sea water and the spreading on the continental shelf is observed with SWATH bottom bathymetry measurements, high resolution echo soundings and CTD profiles. The dilution of the saline Mediterranean water as it flows and spreads on the shelf is only 6 psu before reaching the continental slope, where it sinks to a depth appropriate to its density. The Mediterranean effluent is then incorporated in the general circulation of the southwestern Black Sea.. The eastward circulation of the surface water is observed using satellite imagery and shipboard ADCP.

Keywords

Issuing Organization

North Atlantic Treaty Organization
SACLANT Undersea Research Centre
Viale San Bartolomeo 400, 19138 La Spezia,
Italy

[From N. America: SACLANTCEN (New York) APO AE 09613]

Tel: +39 0187 527 361
Fax:+39 0187 524 600

E-mail: library@saclantc.nato.int

Initial Distribution for Unclassified SR-294

Ministries of Defence

DND Canada	10
CHOD Denmark	8
MOD Germany	15
HNDGS Greece	12
MARISTAT Italy	9
MOD (Navy) Netherlands	12
NDRE Norway	10
MOD Portugal	5
MDN Spain	2
TDKK and DNHO Turkey	5
MOD UK	20
ONR USA	32

NATO Commands and Agencies

NAMILCOM	2
SACLANT	3
CINCEASTLANT/ COMNAVNORTHWEST	1
CINCIBERLANT	1
CINCWESTLANT	1
COMASWSTRIKFOR	1
COMMAIREASTLANT	1
COMSTRIKFLTANT	1
COMSUBACLANT	1
SACLANTREPEUR	1
SACEUR	2
CINCNORTHWEST	1
CINCSOUTH	1
COMEDCENT	1
COMMARAIRMED	1
COMNAVSOUTH	1
COMSTRIKFORSOUTH	1
COMSUBMED	1
NC3A	1
PAT	1

Scientific Committee of National Representatives

SCNR Belgium	1
SCNR Canada	1
SCNR Denmark	1
SCNR Germany	1
SCNR Greece	1
SCNR Italy	1
SCNR Netherlands	2
SCNR Norway	1
SCNR Portugal	1
SCNR Spain	1
SCNR Turkey	1
SCNR UK	1
SCNR USA	2
SECGEN Rep. SCNR	1
NAMILCOM Rep. SCNR	1

National Liaison Officers

NLO Canada	1
NLO Denmark	1
NLO Germany	1
NLO Italy	1
NLO Netherlands	1
NLO Spain	1
NLO UK	1
NLO USA	1

Sub-total	189
SACLANTCEN	30
Total	219